# Trends in seasonal mean speciated aerosol composition in remote areas of the United States from 2000 through 2021

J. L. Hand[1,*], A. J. Prenni[2], and B. A. Schichtel[2]

[1]Cooperative Institute for Research in the Atmosphere, Colorado State University, Fort Collins, CO

[2]National Park Service, Air Resources Division, Lakewood, CO

*Corresponding author:

Dr Jenny Hand
CIRA
1375 Campus Delivery
Colorado State University
Fort Collins, CO 80523 USA
970-491-3699
jlhand@colostate.edu

Index Terms
0305 Aerosols and particles
0365 Troposphere: composition and chemistry

Keywords: aerosol trends, IMPROVE, aerosol composition, seasonality, remote United States

Key Points.

1. Fine mass seasonal mean concentrations have significantly decreased in remote regions of the U.S. in response to regulatory activity.

2. Sulfate aerosols have decreased at the highest rate, followed by nitrate, elemental carbon, fine dust, and organic carbon.

3. Flat and insignificant trends in organic carbon and fine mass at western sites in summer/fall were influenced by biomass smoke emissions.

## Abstract

Large reductions in anthropogenic emissions of particulate matter and its precursor emissions have occurred since the enactment of the Clean Air Act Amendments of 1990. The Interagency Monitoring of Protected Visual Environments (IMPROVE) network has measured $PM_{2.5}$ gravimetric mass (mass of particles with aerodynamic diameters less than 2.5 μm, also referred to here as fine mass, "FM") and speciated $PM_{2.5}$ aerosol composition at remote sites since 1988. Measured species include inorganic anions such as sulfate, nitrate, and chloride, carbonaceous aerosols such as organic (OC) and elemental carbon (EC), and elemental concentrations used to derive fine dust (FD). Trend analyses of seasonal and annual mean mass concentrations were calculated from 2000 through 2021, a period that includes the largest reductions in emissions. On average, annual mean FM at remote sites in the continental United States has decreased at a rate of -1.8% $yr^{-1}$. This reduction is largely due to annual mean trends in sulfate (-6.1% $yr^{-1}$), nitrate (-2.7% $yr^{-1}$), EC (-2.2% $yr^{-1}$), FD (-1.3% $yr^{-1}$), and OC (-0.9% $yr^{-1}$), although the OC annual mean trend was insignificant. Seasonal and regional FM trends varied significantly, with strong reductions in the East in all seasons due to sulfate reductions, and flat and insignificant trends in summer and fall in the West due to the impacts of biomass burning emissions on OC trends. Evaluating regional and seasonal trends in aerosol composition helps identify sources that continue to adversely impact air quality and hinder progress in FM reductions due to successful regulatory activity.



## Plain Language Summary

Particulate matter in the atmosphere is made up of many species that have both anthropogenic and natural sources. Thanks to the Clean Air Act Amendments of 1990, anthropogenic emissions that lead to some particulate matter have decreased, which has resulted in measureable improvements in air quality in remote regions of the United States. Evaluating trends in aerosol measurements from a large-scale monitoring network over the past two decades has shown that at remote sites in the United States, some aerosol species, like sulfates, nitrates, and some carbonaceous aerosols, have decreased significantly due to the emission reductions; but others, like mineral dust and carbonaceous aerosols from wildfire smoke, have not. In order to continue to make progress in improving air quality in the United States, targeting future sources for

emission reductions will require plans to mitigate emissions from these natural sources. Dust and wildfire smoke contributions to particulate matter in remote locations is now a larger fraction compared to two decades ago, and will likely continue to grow with climate change.

## 1. Introduction

The major constituents of $PM_{2.5}$ particulate matter (particles with aerodynamic diameters less than 2.5 μm, referred to here as fine mass, "FM") in the remote and rural United States include inorganic species such as sulfate and nitrate, carbonaceous aerosols such as organic carbon (OC) and elemental carbon (EC), fine mineral dust aerosols (FD), and sea salt. These species have different sources, lifetimes, and seasonality, and influence air quality on local to global scales. They also have different and wide-ranging impacts on visibility (e.g., Hand et al., 2020), climate (e.g., Samset et al., 2018), health (e.g., Shiraiwa et al., 2017), cloud processes (e.g., Seinfeld et al., 2016), and ecology (e.g., Field et al., 2010), among others. These impacts are more accurately estimated when FM and its contributing species are measured concurrently.

Sulfate is a major contributor to FM in the United States and the majority of sulfate in the atmosphere is produced through chemical reactions of sulfur dioxide ($SO_2$). Anthropogenic $SO_2$ is emitted through industrial activities including coal and diesel fuel combustion. Regions that host electric utilities and industrial boilers (e.g., the eastern United States) tend to have the highest $SO_2$ emissions. Oxidation of $SO_2$ to particulate sulfate occurs through homogeneous and heterogeneous reactions, with aqueous chemistry being the most efficient. The degree of acidity of sulfate (from acidic sulfuric acid to fully neutralized ammonium sulfate) depends on the environmental conditions and availability of ammonia to neutralize the sulfuric acid formed from $SO_2$. Sulfate acidity varies spatially and temporally, with recent studies showing that in the East, sulfate is in a more acidic form than in the West (Hidy et al., 2014; Kim et al., 2015; Lowenthal et al., 2015; Weber et al., 2016; Silvern et al., 2017; Lawal et al., 2018; Chen et al., 2019).

Fine particulate nitrate, often in the form of ammonium nitrate, is created from the reversible reaction of gas-phase ammonia and nitric acid. Sources of oxidized nitrogen include combustion of fossil fuels from point sources, including coal-fired powered plants and mobile sources. Other important sources of oxidized nitrogen include biomass burning, lightning, and biogenic sources in soil (Vitousek et al., 1997). Ammonia is primarily emitted from agricultural activities, but mobile sources and natural emissions can also be significant contributors. Lower temperatures

and higher relative humidity favor particulate ammonium nitrate formation. The central United States is an area of high agricultural activity and is associated with high nitrate and ammonium concentrations that can lead to elevated fine-mode ammonium nitrate concentrations (Pitchford et al., 2009; Heald et al., 2012; Warner et al., 2017; Hu et al., 2020).

Organic carbon (OC) aerosols come from both incomplete combustion and reactions of volatile organic carbon (VOC) compounds from biogenic and other sources and are therefore influenced by both anthropogenic and natural sources. The sources of OC in the atmosphere are both primary emissions and secondary formation. Primary emissions include particle mass emitted directly from combustion of fossil fuels or biomass. Secondary organic aerosol formation results from the oxidation of gas-phase precursors from both anthropogenic and biogenic sources. Elemental carbon (EC), also referred to as light absorbing carbon or black carbon depending on the measurement method (Petzold et al., 2013), is emitted directly from incomplete combustion of fossil fuels or biomass (e.g., Bond et al., 2013).

Sources of mineral dust in the atmosphere include both natural and anthropogenic sources, including entrainment from deserts, paved and unpaved roads, agricultural activity, construction, and fire. The seasonal and spatial variability of dust in the United States is influenced by both local, regional, and long-range transport. Several studies have shown that contributions of Asian dust to U.S. fine dust concentrations can be significant episodically, affecting aerosol concentrations and mineralogy across the United States, typically in the spring (e.g., Husar et al., 2001; Prospero et al., 2002; Creamean et al., 2014; Hand et al., 2017; Kim et al., 2021). Transport of North African dust to the United States occurs regularly in summer, affecting aerosol concentrations in the Virgin Islands and the eastern and southeastern United States (Perry et al.,1997; Hand et al., 2017; Bozlaker et al., 2019; Aldhaif et al., 2020; Prospero et al., 2021). Dust concentrations in desert regions of the Southwest arise from local and regional sources as well as transboundary transport from the Chihuahuan desert in Mexico, especially in winter and spring (Rivera et al., 2009; Tong et al., 2012; Hand et al., 2016; Hand et al., 2017). Dust in the central United States is influenced by agricultural activity (Hand et al., 2017; Pu and Ginoux, 2018; Lambert et al., 2020).

Sea salt can be a significant fraction of FM many coastal locations, as well as contribute significantly to light scattering (e.g., Lowenthal and Kumar, 2006; Murphy et al., 2019). Sea salt

concentrations are typically computed from sea salt markers like sodium ion, chloride ion, or combination of ions (White, 2008). Issues can arise when using the chloride ion or chlorine to estimate sea salt, due to depletion of chloride from the reaction of gaseous nitric acid with sea salt that produces sodium nitrate particles and the release of gaseous hydrochloric acid.

Many earlier studies have demonstrated that aerosol composition in the United States has changed in response to the enactment of the Clean Air Act Amendments of 1990 that regulated emissions of gaseous precursors such as $SO_2$ and nitrogen oxides (NOx). These reductions led to decreases in secondary aerosols such as sulfate and nitrate concentrations and deposition (Malm et al., 2002; Lehmann and Gay, 2011; Hand et al., 2012a; Blanchard et al., 2013; Ellis et al., 2013; Attwood et al., 2014; Du et al., 2014; Sickles and Shadwick, 2015; Beachley et al., 2016; Lawal et al., 2018; Zhang et al., 2018; Nopmongcol et al., 2019; Feng et al., 2020). OC concentrations in the eastern United States have declined due to reductions in emissions (Blanchard et al., 2016; Ridley et al., 2018). However, biomass smoke emissions have been shown to influence trends in high concentrations of OC and FM (McClure and Jaffe, 2018). Trends in FD are influenced by large-scale climate variability (Hand et al., 2016; Pu and Ginoux, 2018), and local and regional drought conditions (e.g., Achakulwisut et al., 2019), as well as land-use change (Lambert et al., 2020).

FM trend analysis quantifies the changes in FM concentrations over time, but linking changes in FM to source emissions requires trend analyses of speciated composition. Because speciated aerosols have different sources, with varying seasonal, local, and regional impacts, analyzing seasonal mean trends is important for understanding how changes in emission sources impact air quality. Data from long-term monitoring networks are crucial for evaluating changing concentrations and identifying their relationships to emission sources. Speciated aerosol data from remote and rural sites in the Interagency Monitoring for Protected Visual Environments (IMPROVE) network were used to evaluate trends of seasonal and annual mean concentrations in sulfate, nitrate, OC, EC, and FD from 2000 through 2021. The spatial and seasonal variability in speciated trends were compared to FM trends and emission sources to identify the influence of different sources on FM trends. Identifying impacts from a particular species on FM trends can aid management strategies that target specific sources.

## 2. Methods

The IMPROVE network has been operating since 1988 with the main purpose of tracking trends in aerosol composition and haze in remote areas of the United States (Malm et al., 1994). In 2000 the network expanded in support of monitoring for the Environmental Protection Agency's (EPA) Regional Haze Rule. The IMPROVE network currently operates around 160 mostly remote and rural sites across the United States. Aerosol filters are collected for 24 h (midnight to midnight local standard time) every third day and concentrations are reported at local ambient conditions. Filters are analyzed for inorganic ions using ion chromatography, carbonaceous aerosols using Thermal Optical Reflectance (TOR, Chow et al., 2007), and elemental concentrations using X-Ray fluorescence (XRF). Changes to the network monitoring and analysis have occurred over time; these changes are reported by Hand et al. (2019; 2023) and through data advisories on the IMPROVE website. Additional analysis and monitoring information, including site locations, can be found in Hand et al. (2023). Daily aerosol data from 2000 through 2021 were downloaded for only remote/rural sites from the Federal Environmental Database (FED) on 11 April 2023, including FM, sulfate, nitrate, OC, EC, and elemental species. While sea salt can contribute significantly to particulate matter (PM), especially at coastal sites, it was not considered here due to filter blank contamination in the early 2000s that may influence trends (Hand et al., 2019; Zhang, 2019).

Gravimetric mass measurement is an operationally defined analysis and may have sampling or analytical artifacts that can influence FM trends. For example, nitrate loss and volatilization of some organic species contribute to negative artifacts (e.g., Hering and Cass, 1999; Chow et al., 2005; Watson et al., 2009; Chow et al., 2010), while positive artifacts include retention of water associated with hygroscopic species (Frank, 2006; Hand et al., 2019). Beginning in 2011, higher laboratory relative humidity during weighing resulted in an increase in particle bound water associated with FM data (White, 2016). This issue was resolved in 2019, but it may influence trends in FM (Hand et al., 2019). Seasonal variability of species that are associated with FM biases may confound interpretation of seasonal mean trends in FM.

To reduce impacts from missing data on trend results, missing sulfate concentrations were replaced with sulfur concentrations scaled to sulfate mass (3 × sulfur, Hand et al., 2012a). IMPROVE nitrate ion concentrations at many sites fell below historical values during winter

months from 1996 through 2000; the cause remains unknown (McDade, 2004; 2007). Nitrate concentrations returned to normal levels after 2000, after which the data were deemed valid. Given the number of sites influenced by this anomaly (Debell, 2006), nitrate ion data were considered invalid during winter months of 2000.

Trends in OC and EC may be affected by changes in analytical methods. A review of carbonaceous measurements in the IMPROVE program identified shifts in analytical methods and their impacts on the fraction of EC to total carbon (OC + EC), i.e., EC/TC (Schichtel et al., 2021). One such shift occurred with hardware upgrades in 2005 that resulted in changes in the split between OC and EC derived from the TOR measurement that introduced uncertainty to trend analyses (Chow et al., 2007; White, 2007). Other shifts in EC/TC have also occurred over the history of the program due to new analyzers, new calibrations, and undetermined reasons. EC trends are also affected by hardware and analytic changes, similar to issues that affect OC trends. In addition, Malm et al., (2020) suggested EC may be inadvertently and incorrectly assigned to the OC fraction during the TOR analysis, resulting in an underestimate of true EC concentrations. As discussed by Schichtel et al. (2021), EC concentrations have decreased at rural sites to the point that many sites have concentrations that are below the lower quantifiable limits (LQL, defined as 3 × minimum detection level (MDL)). From 2017 to 2019, about 30% of all EC concentrations were below the LQL. More sites in the West were below LQL than in the East (Schichtel et al., 2021). These low concentrations can lead to difficulties in tracking trends, especially for very low concentrations.

FD concentrations are estimated by summing the oxides of elements typically associated with soil, with a correction for other compounds such as carbonates (Malm et al., 1994). Elemental concentrations are multiplied by factors that account for mass concentrations of the oxide forms. FD concentrations were increased by 15% to reflect biases identified by Hand et al. (2019) (Equation 1).

$$FD = 1.15 \times (2.2 \times [Al] + 2.49 \times [Si] + 1.63 \times [Ca] + 2.42 \times [Fe] + 1.94 \times [Ti]) \quad (1)$$

The analytical methods used to determine elemental concentrations have evolved over time (Hyslop et al., 2015). In 2011, the analysis method switched to the PANalytical XRF system that resolved issues related to undetected Al with concentrations above the MDL (White, 2006). Before 2011, XRF data below the MDL were replaced by 0.5 × MDL. Changes in analytical

methods may not equally affect data for each FD species; therefore, the integrated FD concentration calculated with equation 1 may be less susceptible to possible variability introduced by the analytical methods, although this has not been specifically demonstrated.

All species concentrations are reported with adjustments for blank corrections (Hand et al., 2023). With the exception of data derived from XRF, data were used as reported, i.e., no substitutions were performed for data below MDLs.

Seasonal mean concentrations were calculated for winter (DJF), spring (MAM), summer (JJA), and fall (SON) from 2000 through 2021. December data from the previous year were included in winter mean calculations. Fifty percent of daily data was required for a valid seasonal mean, and annual means were calculated from four valid seasonal means. Trends required 70% of the valid seasonal and annual means over the time period for data from a site to be included in trend calculations, resulting in around 130 to 140 sites, depending on season and species. Data were also aggregated over a four year period (2018–2021) to evaluate the current status in speciated concentrations; for annual mean concentrations, roughly 152 sites met the completeness criteria, depending on species.

A Theil regression was performed with the concentration data as the dependent variable and the year as the independent variable. Theil regressions avoid heavy influence by outliers on the regression results (Theil, 1950). Kendall tau statistics were used to determine the statistical significance, assuming the slope was statistically significant at 5% ($p \leq 0.05$), meaning that there was a 95% chance that the slope was not due to random chance. Trends (% $yr^{-1}$) were calculated by dividing the slope by the median concentration value over the time period of the trend, multiplied by 100%. Reporting trends instead of slopes normalizes the range in concentrations that occur across the United States. However, trends can be large when median concentrations are very low. Site-specific annual mean aggregated concentrations and seasonal mean trend results were interpolated to provide isopleths to guide the eye (Isaaks and Mohan Srivastava, 1989).

Regional mean trends were calculated for ten regions of the United States. Sites were grouped by their state into the following regions: Northeast, Southeast, Midsouth, Central, Southwest, Northwest, California, Alaska, Hawaii, Virgin Islands (see Table 1) and the continental United States (CONUS). The Virgin Islands region included one site. The regions were qualitatively

241 determined based on spatial patterns in FM trends and serve only as a means for summarizing
242 trends. Regional mean trends were computed by aggregating site-specific seasonal mean
243 concentrations for a given region and year and then performing a Theil regression on regional
244 mean concentrations. Sites that met the 70% completeness criterion for a given species and
245 season were included in the regional trend calculation. Regional mean trends were calculated for
246 seasonal and annual means. Periods for regional trends were shortened (2002 through 2021)
247 relative to site-specific trends to limit influences of biases due to sites coming on-line during the
248 early years of network expansion in 2000 (Schichtel et al., 2011; Hand et al., 2014).

249 Table 1. Regions and states (abbreviations) used for regional mean trends. Sites within listed
250 states were included in the corresponding region.

| **Region** | **State Abbreviation** |
|---|---|
| Northeast | ME, NH, VT, MA, RI, CT, NY, PA, NJ, DE, MD, OH, WV, VA, IN, KY |
| Southeast | TN, NC, SC, MS, LA, AL, GA, FL |
| Midsouth | OK, LA, AR |
| Central | ND, SD, MN, MI, WI, IL, MO, KS, NE, IA |
| Southwest | NV, UT, CO, NM, AZ, TX |
| Northwest | WA, OR, ID, MT, WY |
| California | CA |
| Alaska | AK |
| Hawaii | HI |
| Virgin Islands | Virgin Islands |

251

252 The EPA reports an annual National Emission Inventory (NEI) for criteria pollutants such as
253 $SO_2$, nitrogen oxides (NOx), and VOCs as a function of source category. Emission data
254 corresponding to all reported categories were downloaded from the NEI database for annual
255 emissions from 1970 through 2022 for the entire United States. Total wildland fire acreage from
256 1983 through 2021 for the United States were downloaded from the National Interagency Fire
257 Center (NIFC) database. Data from 2004 do not include state lands for North Carolina. The
258 Pacific Decadal Oscillation (PDO) indices were downloaded from the National Centers for
259 Environmental Information (NCEI) database. The NCEI index is based on the National Oceanic
260 and Atmospheric Administration's (NOAA) extended reconstruction of sea surface temperatures.
261 PDO indices for all months from 1854 through 2023 are available. Last data access for NEI, burn
262 acreage, and PDO indices was 18 August 2023.

## 3. Fine Mass and Speciated Aerosol Concentrations

The current status in the 2018 through 2021 annual mean $PM_{2.5}$ speciated mass concentrations are shown in Figure 1(a-f) for sulfate, nitrate, OC, EC, FD, and FM, respectively. For each species, the contour levels were created with the highest level corresponding to the 95$^{th}$ percentile in annual mean mass concentration. Isopleths in mass concentration serve to guide the eye for spatial patterns and are not for strict interpretation.

The highest annual mean sulfate ion concentration in the CONUS occurred at sites around the Ohio River valley and the Midsouth (~1 μg m$^{-3}$) (see Figure 1a). Sulfate concentrations decreased sharply at sites toward the western United States, where concentrations were less than 0.5 μg m$^{-3}$, with the lowest concentrations at sites in the Northwest and Intermountain West. Concentrations in the West reflected lower $SO_2$ emissions that lead to secondary particulate sulfate (Hand et al., 2020). Somewhat higher concentrations occurred at sites in southern California, and at sites in the Northern Great Plains. Concentrations in the northwestern United States were less than 0.3 μg m$^{-3}$, indicating transboundary contributions were lower than previous modeling studies suggest (Park et al., 2004; 2006) possibly due to reduced emissions in Asia (Shi et al., 2022).

The spatial pattern in nitrate differed from sulfate in that the area of high annual mean nitrate concentrations (~0.9 μg m$^{-3}$) occurred in the central United States (Figure 1b) where intensive agricultural activity occurs (Pitchford et al., 2009; Hu et al., 2020). Sites in central and southern California also had higher annual mean nitrate concentrations. Sites with elevated concentrations in northern North Dakota may be associated with oil and gas energy development (e.g., Prenni et al., 2016). High annual mean concentrations were observed at Dinosaur National Monument in Colorado, also likely associated with oil and gas development (Prenni et al., 2022). Concentrations were much lower at sites in the Intermountain West and Northwest, with annual mean concentrations less than 0.3 μg m$^{-3}$. Similarly, low annual mean concentrations occurred at sites in the Southeast and Northeast.

Unlike spatial patterns in sulfate and nitrate, the highest annual mean OC concentrations (> 2 μg m$^{-3}$) occurred at sites in the northwestern United States, and central and northern California, due to the influence of biomass burning (Figure 1c). OC concentrations that are highly influenced by biomass burning are likely underestimated, since the high concentrations can cause filter

clogging and loss of operator support. Elevated levels of OC (1–2 μg $m^{-3}$) also occurred at sites across the eastern United States, likely associated with biogenic and anthropogenic emissions (e.g., Blanchard et al., 2016). Annual mean concentrations were lowest at sites in the Southwest (< 1 μg $m^{-3}$).

The spatial pattern in annual mean EC concentrations was similar to OC, especially at sites in the western United States where biomass smoke emissions have influenced both species (Figure 1d). Annual mean EC was over 0.4 μg $m^{-3}$ at many of these sites. EC concentrations were also elevated (~ 0.2–0.3 μg $m^{-3}$) at sites across the eastern United States, many coinciding with sites that had high OC. Concentrations were relatively low at sites across the Southwest and Intermountain West (< 0.2 μg $m^{-3}$).

Unlike the east-west gradient observed for sulfate, nitrate, OC, and EC, annual mean FD concentrations exhibited a north-south gradient with higher concentrations at sites in the southern United States. Dust concentrations in desert regions of the Southwest are expected to be higher due to the impacts of local and regional sources (e.g., Tong et al., 2012; Hand et al., 2017). FD in the central United States is influenced by agricultural activity (Pu and Ginoux, 2018; Lambert et al., 2020), and FD at sites in the Southeast is influenced by transport of dust from North Africa (Aldhaif et al., 2020). The highest annual mean concentrations were observed at sites in the Southwest (>1.5 μg $m^{-3}$). Concentrations of FD at sites in the northern United States were typically less than 0.5 μg $m^{-3}$, with the exception of higher FD concentrations near Columbia River Gorge, Washington and at sites in northern Montana and North Dakota.

The spatial pattern of 2018–2021 annual mean FM concentrations reflected the combined patterns of of sulfate, nitrate, OC, and FD (see Figure 1f). The highest concentrations of annual mean FM (> 5 μg $m^{-3}$) occurred at sites in the central and eastern United States, likely due to impacts from sulfate, nitrate, and OC. Similarly, high FM concentrations at sites in the West were likely due to impacts from OC. The lowest FM concentrations occurred at sites in the Intermountain West, where speciated concentrations were relatively low. The highest annual mean FM concentration was 9.7 μg $m^{-3}$ at Sequoia National Park, California, which is below the current annual primary National Ambient Air Quality Standard (NAAQS) of 12 μg $m^{-3}$, but near the new proposed standard of 9-10 μg $m^{-3}$.

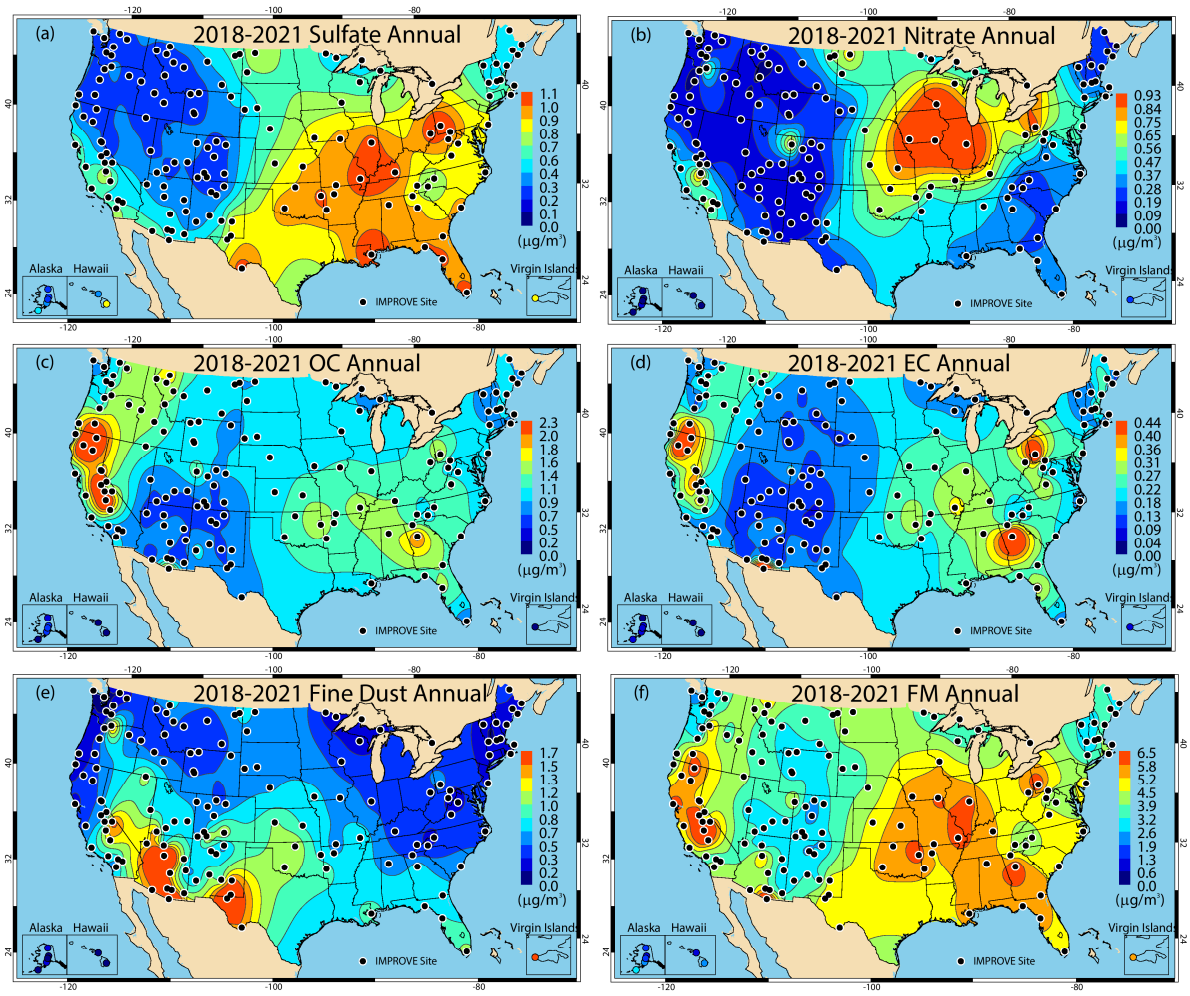


Figure 1. IMPROVE 2018–2021 annual mean $PM_{2.5}$ concentrations (µg $m^{-3}$) for (a) sulfate ion, (b) nitrate ion, (c) organic carbon, (OC) (d) elemental carbon (EC), (e) fine dust (FD), and (f) gravimetric fine mass (FM).

Changes in FM depend on the species that compose it. Timelines of regional, annual mean mass concentrations for ammonium sulfate (AS), ammonium nitrate (AN), particulate organic matter (POM), EC, and FD are shown in Figure 2 (a-j) for the summary regions defined in Section 2. For only this figure, mass correction factors were applied to individual species in order to represent contributions to total FM. Sulfate was assumed to be fully neutralized ammonium sulfate (AS=1.375 × sulfate ion) and nitrate was assumed to be ammonium nitrate (AN = 1.29 × nitrate ion). A constant organic carbon multiplier of 1.8 was used for the entire year to calculate particulate organic matter (POM=1.8 × OC) to avoid obfuscating seasonal OC trends.

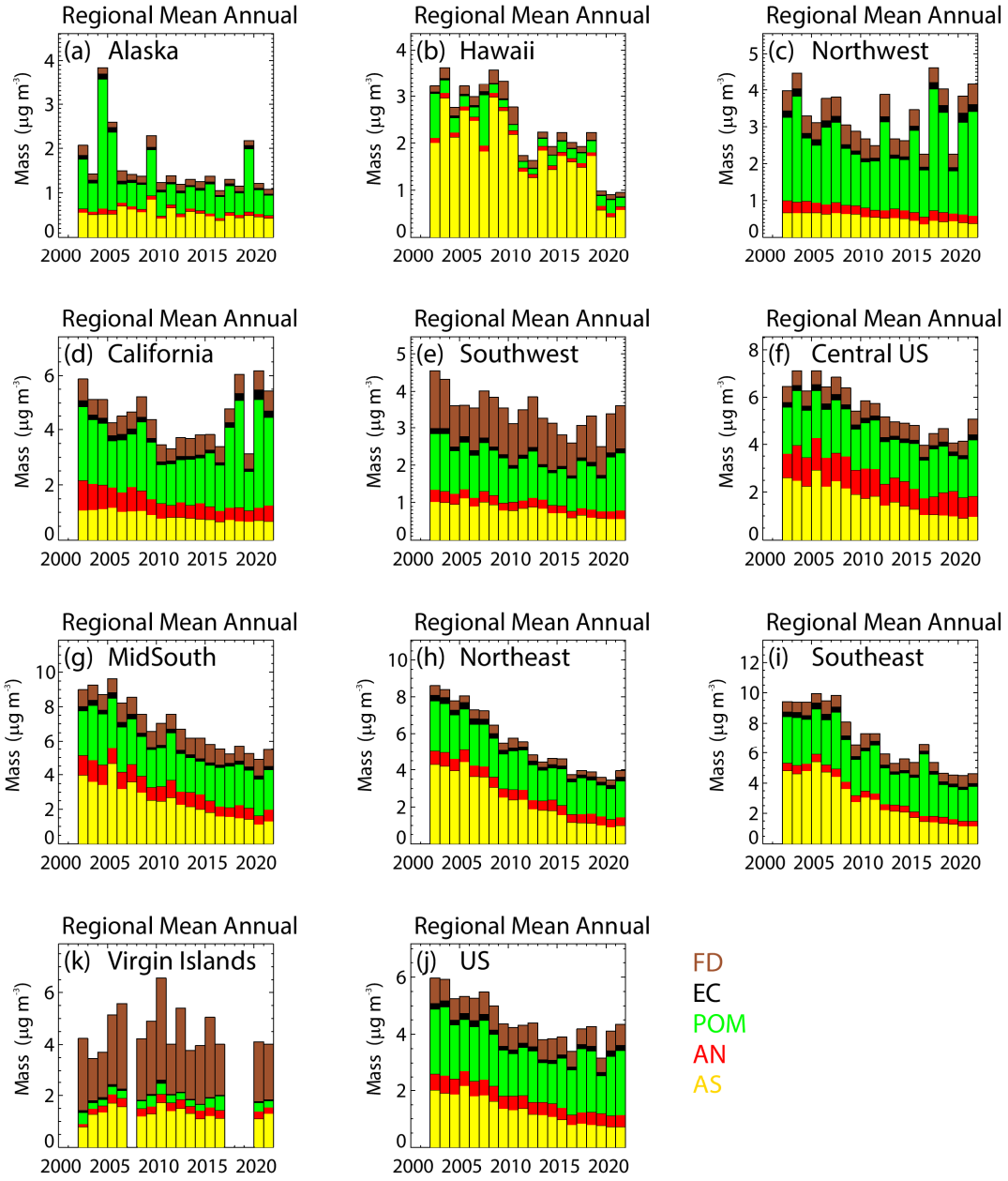


Figure 2. IMPROVE regional, annual mean mass concentrations (µg $m^{-3}$) for ammonium sulfate (AS), ammonium nitrate (AN), particulate organic matter (POM), elemental carbon (EC), and fine dust (FD) for major summary regions.

Species concentrations and contributions to FM varied for each region, and for some regions the contributions have changed over time. For example, AS was a major fraction of FM in the early

2000s, especially in eastern regions such as the Central, Midsouth, Northeast, the Southeast regions (Figure 2f, 2g, 2j, and 2i, respectively). AS concentrations have dramatically decreased in these regions and is a lower contributor to FM on an annual mean basis. Over time, POM has grown in its contribution to FM, although its absolute concentration has decreased, especially at regions in the East. In western regions, POM was a major contributor to FM, and its contributions have increased as contributions from other species, such as AS and AN, have decreased. Impacts from high fire years (2017–2018, 2020–2021) were evident in the Northwest and the California regions (Figure 2c and 2d, respectively), and to a lesser degree in the Southwest region (Figure 2e). FD contributions were highest in the Southwest region, although they were non-negligible at western regions the Northwest and California regions (Figure 2c and Figure 2d, respectively), and even in the Central and Midsouth regions (Figure 2f and 2g, respectively). OCONUS (outside the continental United States) regions were each dominated by different species. The Virgin Islands region was dominated by FD, while the Alaska region had very low FD contributions and instead was dominated by AS and POM. In the Hawaii region, AS is the major contributor to FM, although the reasons for the decrease in AS around 2019 is unknown. For the total CONUS (Figure 2j), the major contributing species has shifted from AS to POM.

## 4.0 Trends

The mass concentration timelines shown in Figure 2 indicate significant changes in speciated composition, as well as FM, over the past two decades. Trend analyses provide a quantitative investigation of the observed changes.

### *4.1 Gravimetric Fine Mass*

Trends in FM are driven by trends in contributing species, depending on the degree of the species' contribution to the fine mass budget. However, inferring FM trends based on the trends of other species is confounded because of the spatial and seasonal variability in trends of a specific species relative to another. The spatial and seasonal variability in FM trends can understood by examining the trends in others major contributing species. In this section, trends in FM first are presented, followed by trends in the species shown in Figure 1. Individual site trends are shown on maps with isopleths in percent per year. Negative trends are shown with

downward-pointing triangles and contoured with cold colors, while positive trends are shown with upward-pointing triangles and warm colors. Statistically significant trends ($p \leq 0.05$) are denoted with filled triangles. Scales were kept similar for all parameters so that trends can be compared. Interpolations in regions without sites should be viewed only as a spatial transition.

Seasonal mean trends in FM are shown in Figure 3(a-d). The strongest reductions in FM occurred at sites in the eastern United States, especially in summer and fall (Figures 3c and 3d, respectively), with trends around -6% $yr^{-1}$ to -7% $yr^{-1}$. The strongest reduction of -7.6% $yr^{-1}$ ($p < 0.001$) occurred in summer in Frostburg Reservoir, Maryland (site code, FRRE1) and of -6.3% $yr^{-1}$ ($p < 0.001$) in fall in Cohutta, Georgia (COHU1). Positive trends in summer and fall occurred in summer in Lava Beds, California (LABE1; 4.9% $yr^{-1}$, $p = 0.040$) and in fall in Jarbidge, Nevada (JARB1; 2.4% $yr^{-1}$, $p = 0.022$). These positive trends at sites in the West are part of a larger, regional pattern of sites across the West with positive but insignificant trends during summer and fall. Insignificant trends also occurred at sites in the Northern Great Plains in spring and California and Oregon in winter. The strong spatial gradient in trends at sites between the East and the West during summer and fall indicated sources with regional influence on FM, such as biomass smoke emissions. During winter and spring the spatial gradient weakened, with negative trends across the United States, and the strongest reductions at sites in the East.

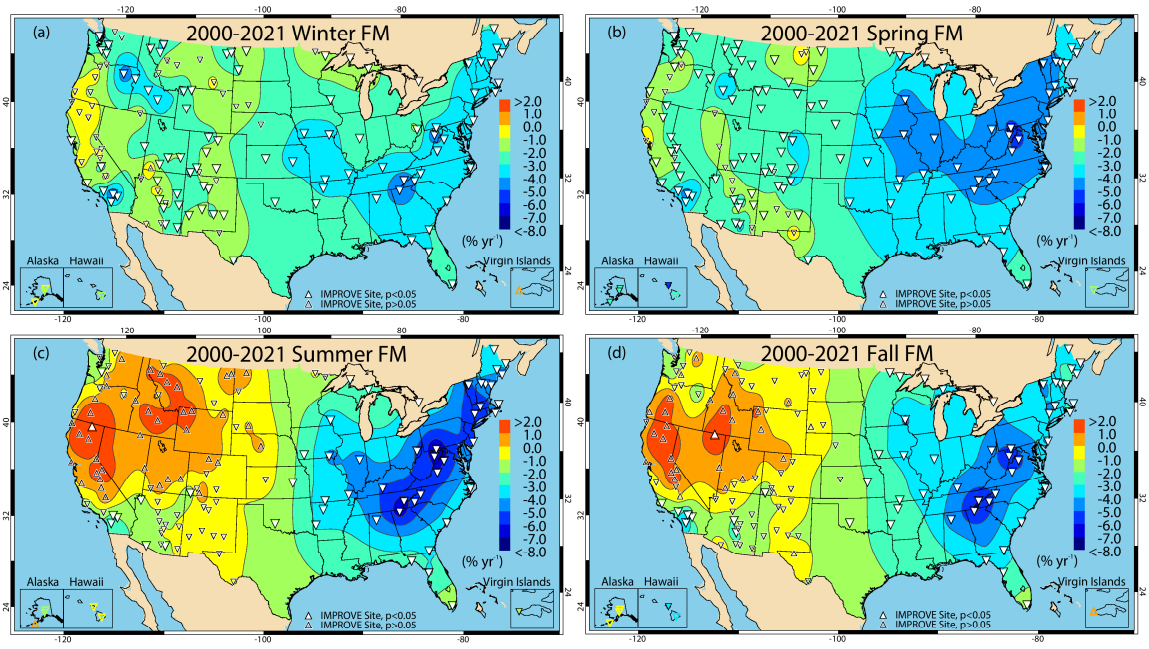


Figure 3. Seasonal mean $PM_{2.5}$ gravimetric fine mass (FM) trends (% $yr^{-1}$) from 2000–2021 for (a) winter (DJF) (b) spring (MAM) (c) summer (JJA), and (d) fall (SON). Filled triangles correspond to statistically significant trends ($p \leq 0.05$).

Statistically significant regional, seasonal mean trends in FM were negative across most U.S. regions (Figure 4). The strongest reductions in FM occurred in the Northeast and Southeast regions during summer (-4% $yr^{-1}$ to -5% $yr^{-1}$) and the weakest seasonal trends occurred in winter (~-3% $yr^{-1}$). Trends in the Midsouth and Central regions were less negative than in eastern regions, with the strongest trends in spring (~-3% $yr^{-1}$). FM decreased significantly during spring and winter at regions in the West; however, summer and fall trends were flat and insignificant, reflecting the spatial patterns seen in Figure 3. The overall annual mean trend for the United States was -1.8% $yr^{-1}$ ($p<0.001$). Timelines for seasonal, regional mean concentrations are shown in the Supplemental Information (Figures S1-S5) and demonstrate the linear decrease in FM concentrations.

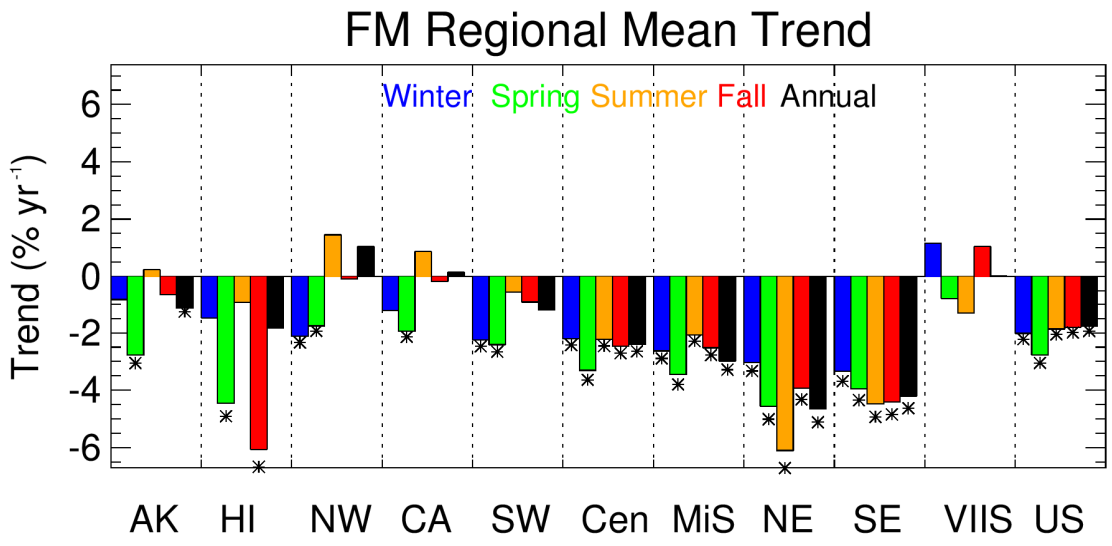


Figure 4. Regional, seasonal mean $PM_{2.5}$ gravimetric fine mass (FM) trends (% $yr^{-1}$) from 2002–2021 for major U.S. regions for winter, spring, summer, fall, and annual means. Regions are arranged from west to east (AK = Alaska, HI = Hawaii, NW = Northwest, CA= California, SW = Southwest, Cen = Central, MiS = Midsouth, NE = Northeast, SE = Southeast, VIIS = Virgin Islands, and U.S. = all continental sites). Statistically significant trends ($p \leq 0.05$) are denoted with "*".

*4.2 Sulfate*

Seasonal mean sulfate ion concentrations decreased significantly across the United States during all seasons (Figure 5a-d). The strongest reductions (-3 to -14% $yr^{-1}$) occurred at sites in the eastern United States, especially in the Appalachian region where $SO_2$ emissions have strongly decreased (Krotkov et al., 2016; Kharol et al., 2017; Feng et al., 2020; Hand et al., 2020). This reduction in sulfate has led to widespread improvements in visibility (Hand et al., 2020) and reductions in sulfate deposition (Sickles and Shadwick, 2015) and reductions have been reported in both rural and urban environments in the East due to the regional influence of sulfate (Hand et al., 2012a; Blanchard et al., 2013). Less progress has occurred for sites in the West, where emissions and concentrations are historically lower than at sites in the East (e.g., Hand et al., 2012a; 2020), and natural and international sources have larger relative contributions. Therefore, the reductions of regulated emissions has had less of an impact on already-low sulfate concentrations. Most trends in the West ranged from -2% $yr^{-1}$ to -5% $yr^{-1}$ during all seasons. The highest number of insignificant trends occurred during winter (Figure 5a) at sites in Montana,

Wyoming, and California. Stronger reductions at sites in the Southwest occurred during winter and fall relative to spring and summer (compare Figures 5a and 5d to Figures 5b and Figure 5c, respectively). Concentrations at sites in southern California decreased more strongly than at sites in central California during all seasons, with the strongest reductions in southern California at the Agua Tibia (AGTI1) site (-5% $yr^{-1}$ to -7% $yr^{-1}$ depending on season). The greatest reductions in seasonal mean sulfate concentrations ranged from -14.5% $yr^{-1}$ ($p < 0.001$) at Frostburg Reservoir, Maryland (FRRE1) in summer and at Cohutta, Georgia (COHU1) in fall (-14.5% $yr^{-1}$, $p < 0.001$). These are the same sites with the strongest reductions in FM. Concentrations significantly increased (1.3% $yr^{-1}$, $p = 0.027$) during summer at Simeonof, Alaska (SIME1).

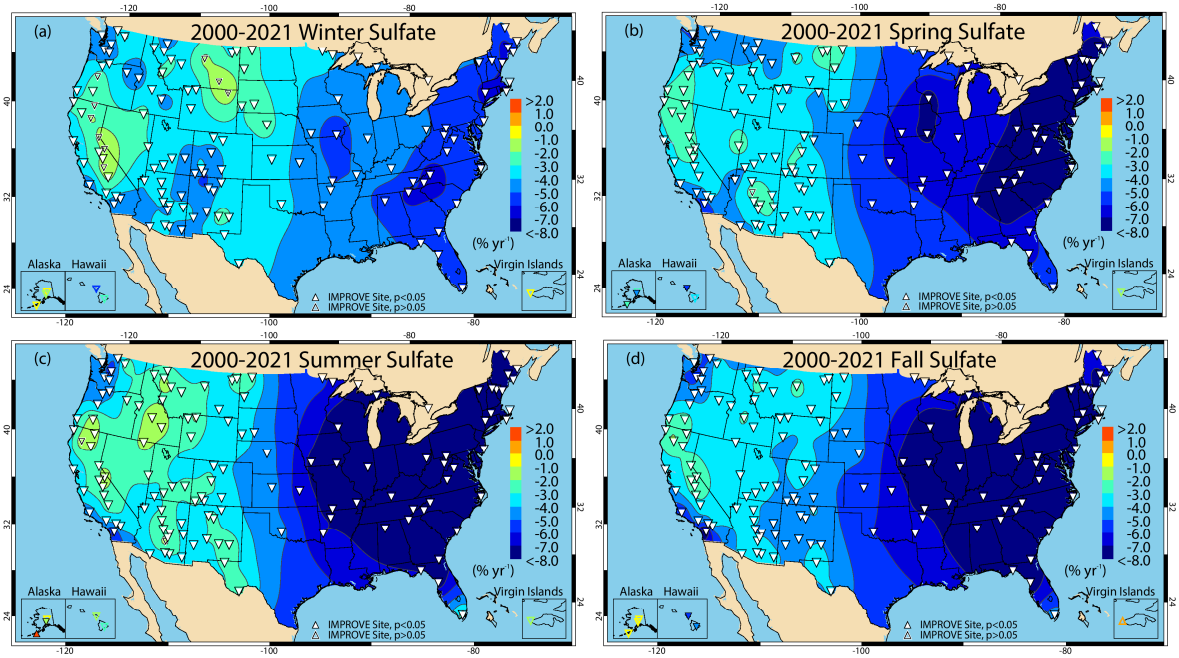


Figure 5. Seasonal mean sulfate ion concentration trends (% $yr^{-1}$) from 2000–2021 for (a) winter (DJF) (b) spring (MAM) (c) summer (JJA), and (d) fall (SON). Filled triangles correspond to statistically significant trends ($p \leq 0.05$).

The spatial gradients and seasonal distribution in sulfate ion trends are summarized in the regional mean trends presented in Figure 6. The largest reductions in seasonal mean sulfate ion concentrations occurred for sites in the Northeast region (-10.5% $yr^{-1}$, $p < 0.001$ in summer), followed by the Southeast region (-8.9% $yr^{-1}$, $p < 0.001$, in fall). These trends were similar to FM regional trends shown in Figure 4. For the Northeast, Midsouth, and Central regions, the largest decrease in sulfate ion concentrations occurred during summer, while in the Southeast

decreases in fall were slightly larger. In all eastern regions the lowest decreases occurred during winter. This difference in seasonal mean trends has led to a decrease in the seasonality of sulfate ion concentrations (Chan et al., 2018)), and may be due to the availability of oxidants (Paulot et al., 2017; Shah et al., 2018). In regions in the western United States, the rate of decrease was ~-3% $yr^{-1}$, roughly half of that in the eastern regions. The differences in seasonal mean trends were also smaller, indicating that sulfate ion concentrations decreased by similar rates across seasons. Summer trends in the Hawaii region were also lower than other seasons. However, overall, across the eastern United States, sulfate ion concentrations have decreased at a higher rate during summer and fall. Seasonal mean trends in Alaska and the Virgin Islands regions were relatively flat and insignificant, with the exception of spring and annual mean trends in the Alaska region. The annual mean sulfate trend across the United States was -6.1% $yr^{-1}$ ($p<0.001$). Timelines of regional and seasonal mean sulfate concentrations are shown in Figures S6-S10.

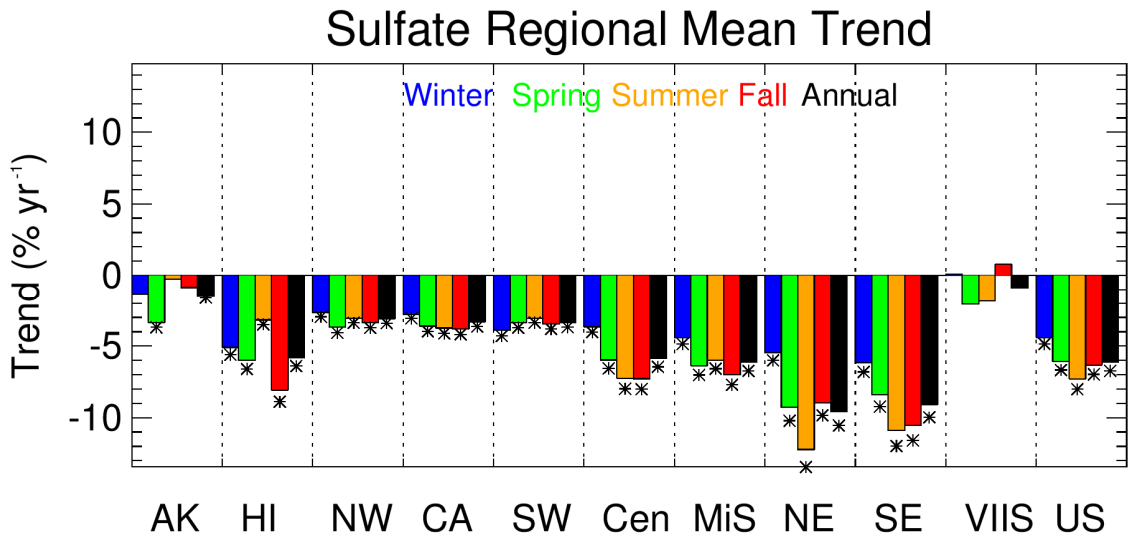


Figure 6. Regional, seasonal mean sulfate ion trends (% $yr^{-1}$) from 2002–2021 for major U.S. regions for winter, spring, summer, fall, and annual means. Regions are arranged from west to east United States (AK = Alaska, HI = Hawaii, NW = Northwest, CA= California, SW = Southwest, Cen = Central, MiS = Midsouth, NE = Northeast, SE = Southeast, VIIS = Virgin Islands, and US = all sites). Statistically significant trends ($p \leq 0.05$) are denoted with "*".

*4.3 Nitrate*

Trends in seasonal mean nitrate ion concentrations are shown in Figure 7(a-d). For all seasons, strong reductions occurred in southern California, at sites like San Gorgonio (SAGO1), Agua

Tibia (AGTI1), and Joshua Tree (JOSH1), where statistically significant trends ranged from -8% $yr^{-1}$ to -11% $yr^{-1}$, depending on season. The Southern California region experienced significant reductions in NOx emissions (Russell et al., 2012; Yu et al., 2021). Nitrate decreased at sites across the western United States and in the Midsouth and central United States, with the strongest reductions (-4% $yr^{-1}$ to -5% $yr^{-1}$) in spring and fall (Figure 7b and 7c, respectively). Insignificant trends occurred at sites across the West during summer (Figure 7c), however concentrations at many of these sites during summer tend to be lower than during cool months with conditions that favor particulate nitrate formation, and the annual mean concentrations shown in Figure 1b were relatively low. At sites in the Northern Great Plains, insignificant trends occurred during all seasons, likely due to the influence of oil and gas development in the region, offsetting reductions in other emission sectors (Hand et al., 2012b; Prenni et al., 2016; Evanoski-Cole et al., 2017; Gebhart et al., 2018)). Seasonal mean trends ranged from -11.0% $yr^{-1}$ ($p < 0.001$) during spring in Joshua Tree, California (JOSH1) and -11.9% $yr^{-1}$ ($p < 0.001$) in San Gorgonio, California (SAGO1) in fall to 1.7% $yr^{-1}$ ($p = 0.016$) in Dolly Sods, West Virginia (DOSO1) in summer and 1.6% $yr^{-1}$ ($p = 0.021$) in the Virgin Islands (VIIS1) in fall.

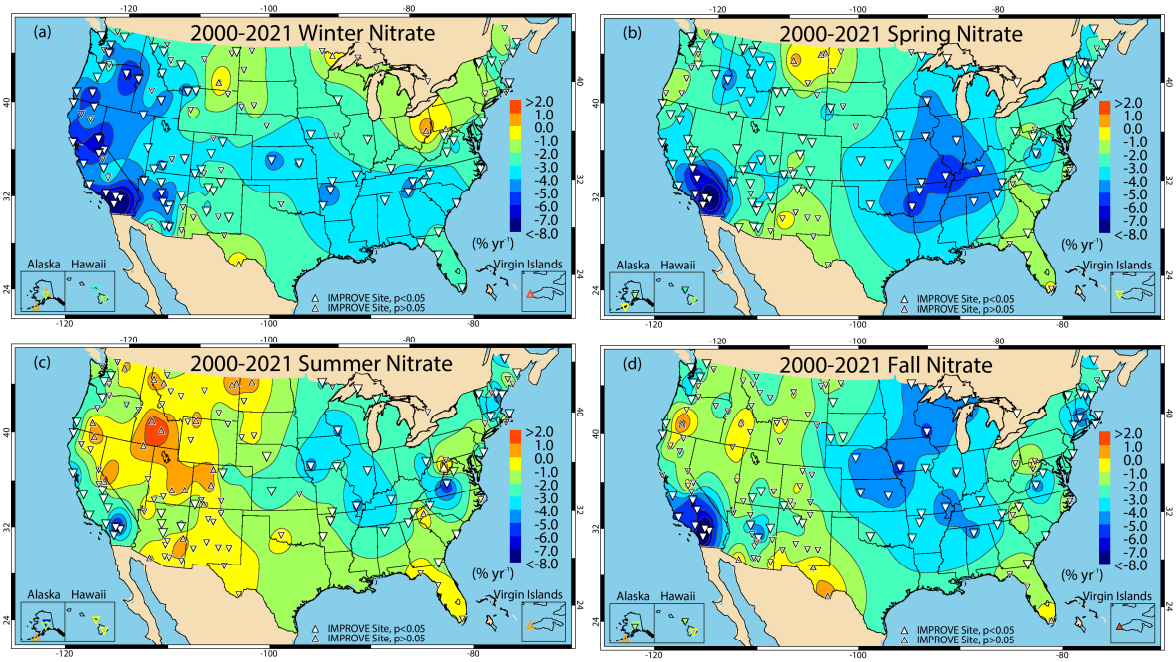


Figure 7. Seasonal mean nitrate ion concentration trends (% $yr^{-1}$) from 2000–2021 for (a) winter (DJF) (b) spring (MAM) (c) summer (JJA), and (d) fall (SON). Filled triangles correspond to statistically significant trends ($p \leq 0.05$).

Comparisons of regional and seasonal mean nitrate trends are shown in Figure 8. The strongest reductions in regional mean nitrate concentrations occurred in the California region, especially in spring (-6.1% $yr^{-1}$, $p < 0.001$) and fall (-5.4% $yr^{-1}$, $p < 0.006$); the lowest trends occurred during summer (-3.6% $yr^{-1}$, $p < 0.002$). A similar seasonal pattern in trends occurred in the Northwest and Southwest regions, although summer trends were insignificant. Other regions had different seasonal variability in trends. Most regions experienced the strongest reductions in winter or spring, with the exception of the Northeast region (similar reductions for all seasons), and the Central region. The Central region had the highest nitrate reductions in fall (-4.8% $yr^{-1}$, $p < 0.001$) with the lowest trends in winter (-2.0% $yr^{-1}$, $p = 0.044$). The OCONUS regions had mostly insignificant trends, with the exception of negative winter and annual mean trends in the Hawaii region, and positive fall mean trends in the Virgin Islands region (1.2% $yr^{-1}$, $p = 0.048$). The range in regional, seasonal mean trends that occurred across the United States indicated potentially different sources and atmospheric processes controlling nitrate concentrations across these regions. The total U.S. annual mean trend in nitrate was -2.7% $yr^{-1}$ ($p < 0.001$), roughly half of the annual mean U.S. sulfate trend. Figures S11-S15 provide timelines of regional, seasonal mean nitrate concentrations.

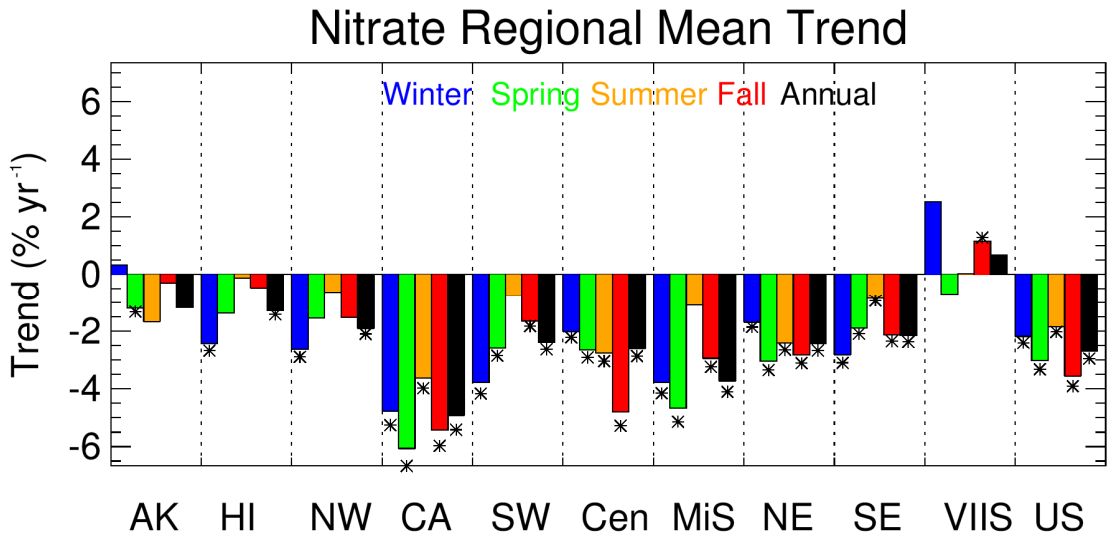


Figure 8. Regional, seasonal mean nitrate ion trends (% $yr^{-1}$) from 2002–2021 for major U.S. regions for winter, spring, summer, fall, and annual means. Regions are arranged from west to east (AK = Alaska, HI = Hawaii, NW = Northwest, CA= California, SW = Southwest, Cen = Central, MiS = Midsouth, NE = Northeast, SE = Southeast, VIIS = Virgin Islands, and US = all sites). Statistically significant trends ($p \leq 0.05$) are denoted with "*".

### *4.4 Organic Carbon*

Seasonal mean trends in OC had much greater spatial variability than sulfate and nitrate trends (Figure 9(a-d)). Relatively strong reductions in OC have occurred at sites in the Southeast during all seasons (-2% $yr^{-1}$ to -4% $yr^{-1}$) due to reductions in anthropogenic emissions (e.g., Blanchard et al., 2016; Malm et al., 2017; Ridley et al., 2018). OC also decreased at sites in the West but only during winter (Figure 9a) and spring (Figure 9b) (-3% $yr^{-1}$ to -4% $yr^{-1}$). Insignificant winter trends, some positive, occurred at sites in the Central Valley of California and northern California, Oregon, and Arizona. The spatial patterns in trends at sites in the West during summer and fall were very different than other seasons. With the exception of sites in southern California and Arizona, many of the sites across the West had insignificant positive trends. These trends indicate sources that regionally influence OC, such as biomass smoke emissions. As McClure and Jaffe (2018) reported, biomass smoke has influenced the highest $PM_{2.5}$ concentrations at sites across the Northwest. In fact, the similarities in spatial patterns between OC and FM trends in summer and fall (recall Figure 3c and 3d, respectively) suggest trends in OC are affecting seasonal and annual mean FM trends, especially since OC is a large fraction of the fine mass budget at sites in the West, as shown for several western regions in Figure 2. The statistically significant OC trends in summer and fall ranged from -5.4% $yr^{-1}$ ($p < 0.001$) in Everglades, Florida (EVER1) to -0.9% $yr^{-1}$ ($p = 0.009$) in Casco Bay, Maine (CABA1). In winter and spring, statistically significant trends ranged from -6.5% $yr^{-1}$ ($p = 0.002$) in White River, Colorado (WHRI1) to -1.1% $yr^{-1}$ ($p = 0.046$) in Ike's Backbone, Arizona (IKBA1).

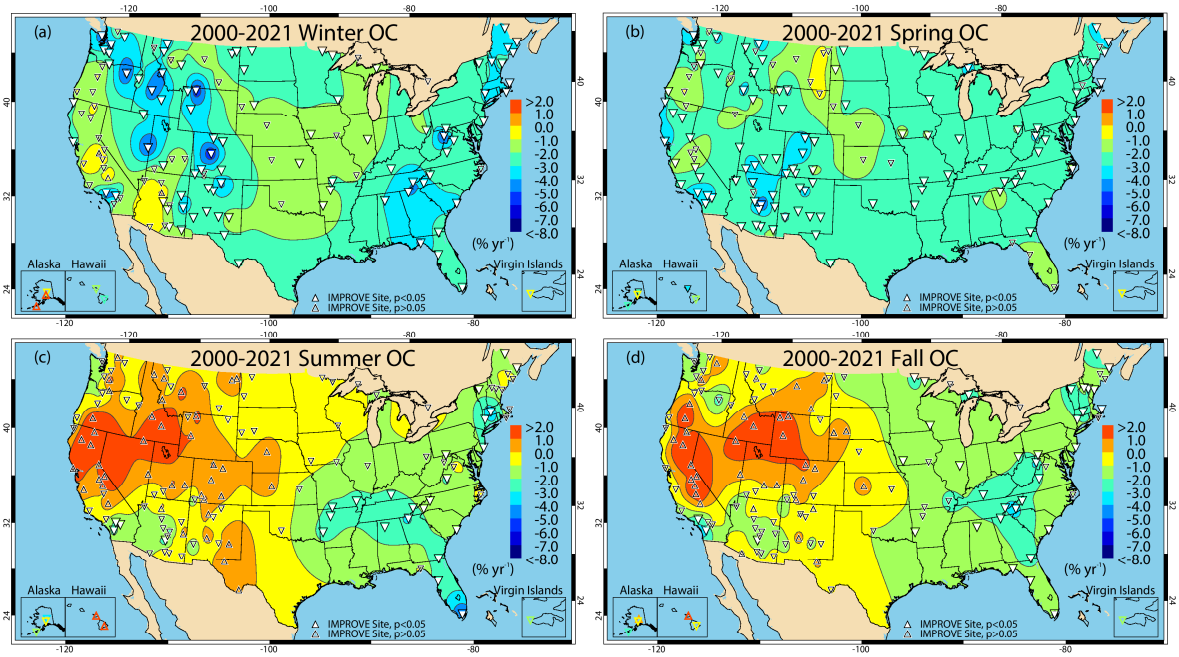


Figure 9. Seasonal mean organic carbon (OC) trends (% $yr^{-1}$) from 2000–2021 for (a) winter (DJF) (b) spring (MAM) (c) summer (JJA), and (d) fall (SON). Filled triangles correspond to statistically significant trends ($p \leq 0.05$).

Regional, seasonal mean OC trends are shown in Figure 10. Statistically significant trends occurred during all seasons in the Northeast and Southeast regions, around -2% $yr^{-1}$ to -3% $yr^{-1}$. The strongest reductions in these regions occurred in winter and spring. Trends in the Central U.S. region were lower than regions in the East (-1% $yr^{-1}$ to -2% $yr^{-1}$) and statistically significant in winter and spring, but insignificant in summer and fall. Seasonal mean trends at western regions were more variable than in the East. Regional mean winter and spring trends were negative and statistically significant in the Northwest, California, and Southwest regions, and OC declined strongly in these seasons (-2% $yr^{-1}$ to -3% $yr^{-1}$), similar to winter trends in eastern regions. However, western regional mean trends in summer and fall were insignificant and flat, especially in the Northwest and California regions. These patterns reflect the site-specific trends in Figure 9 and demonstrate the importance of seasonal sources, such as biomass burning emissions, on OC concentrations across the West. Similar regional and seasonal mean patterns were observed for FM (recall Figure 4). The annual mean OC trend for the United States was insignificant (-0.9% $yr^{-1}$, $p = 0.330$); OC was the only species with an insignificant annual mean U.S. trend. Timelines of these concentrations are found in Figures S16-S20.

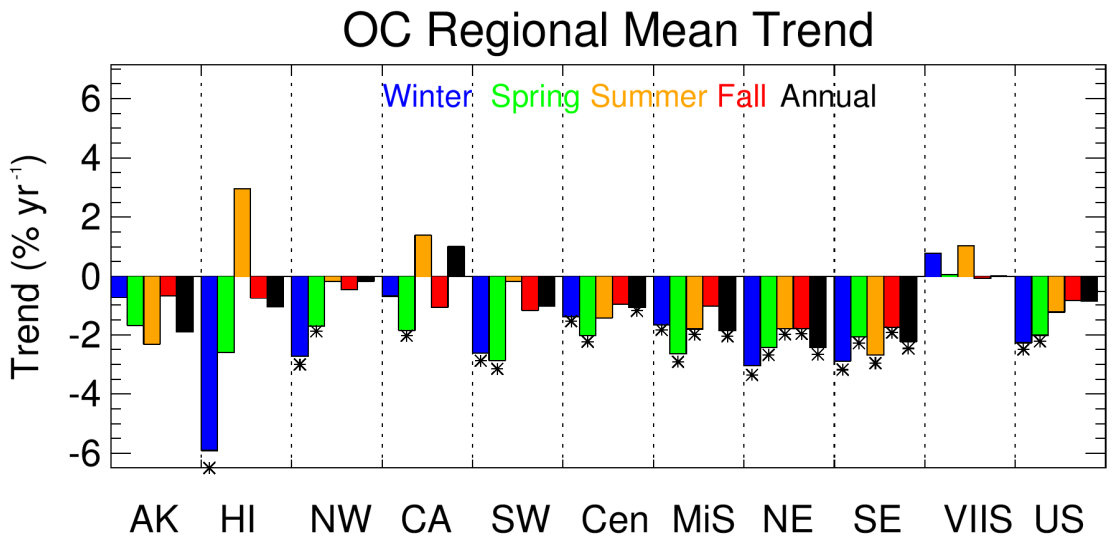


Figure 10. Regional, seasonal mean organic carbon (OC) trends (% $yr^{-1}$) from 2002–2021 for major U.S. regions for winter, spring, summer, fall, and annual means. Regions are arranged from west to east (AK = Alaska, HI = Hawaii, NW = Northwest, CA= California, SW = Southwest, Cen = Central, MiS = Midsouth, NE = Northeast, SE = Southeast, VIIS = Virgin Islands, and US = all sites). Statistically significant trends ($p \leq 0.05$) are denoted with "*".

*4.5 Elemental Carbon*

The spatial patterns in seasonal mean EC trends were somewhat similar to OC trends (Figure 11(a-d)), especially with strong reductions at sites in the western United States in winter and spring (Figure 11a and 11b, respectively). Trends during winter and spring ranged from -8.8% $yr^{-1}$ ($p < 0.001$) at San Gabriel, California (SAGA1) to -1.4% $yr^{-1}$ ($p < 0.001$) at Medicine Lake, Montana (MELA1). Insignificant trends at sites in northern Montana and North Dakota are likely influenced by oil and gas development (Gebhart et al., 2018). At sites in the East, EC decreased significantly across the region during all seasons, but especially in summer (Figure 11c). However, in the West, trends in EC in summer and fall (Figure 11c and 11d, respectively) were mostly statistically insignificant, similar to insignificant trends for OC, and were likely also influenced by biomass smoke. Trends during summer and fall ranged from -7.1% $yr^{-1}$ ($p < 0.001$) at San Gorgonio, California (SAGO1) to 2.5% $yr^{-1}$ ($p = 0.045$) at Guadalupe Mountains, Texas (GUMO1). Guadalupe Mountains is near areas with oil and gas development, and these emissions have influenced air quality at nearby sites (Benedict et al., 2020; Naimie et al., 2022).

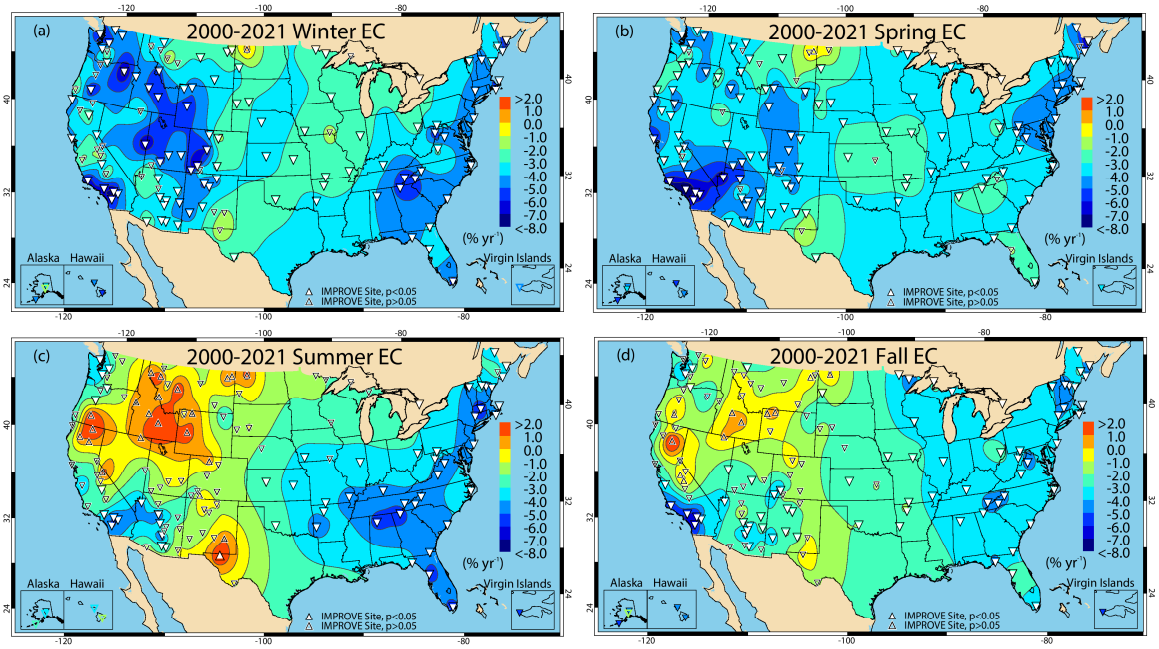


Figure 11. Seasonal mean elemental carbon (EC) trends (% $yr^{-1}$) from 2000–2021 for (a) winter (DJF) (b) spring (MAM) (c) summer (JJA), and (d) fall (SON). Filled triangles correspond to statistically significant trends ($p \leq 0.05$).

Regional, seasonal mean trends are summarized in Figure 12 and corresponding timelines are shown in Figures S21-S25. Negative, and mostly statistically significant trends occurred for all regions and seasons, with the exception of summer and fall trends in western regions, such as the Northwest, California, and the Southwest regions. In these regions, negative and statistically significant winter and spring trends (-4% $yr^{-1}$ to -5% $yr^{-1}$) contrasted the insignificant and flat trends in EC during summer and fall, likely reflecting the influence of biomass smoke on EC concentrations. This pattern shifts for the Central region, with similar magnitudes in statistically significant trends during all seasons (~-2% $yr^{-1}$). In eastern regions, stronger reductions were observed during summer (~-4% $yr^{-1}$), contrasting summer trends in western regions. Summer mean EC trends in Hawaii were flat and insignificant, but EC decreased strongly in other seasons. The difference in seasonal and regional trends across the United States implies different sources that influenced EC depending on region and season, especially with respect to East versus West, and summer versus winter. The success of regulatory activity that led to reductions of EC in the East (Murphy et al., 2011; Hidy et al., 2014; Blanchard et al., 2016) contrasts the

impacts of biomass smoke emissions that hindered similar progress in summer in regions of the West.

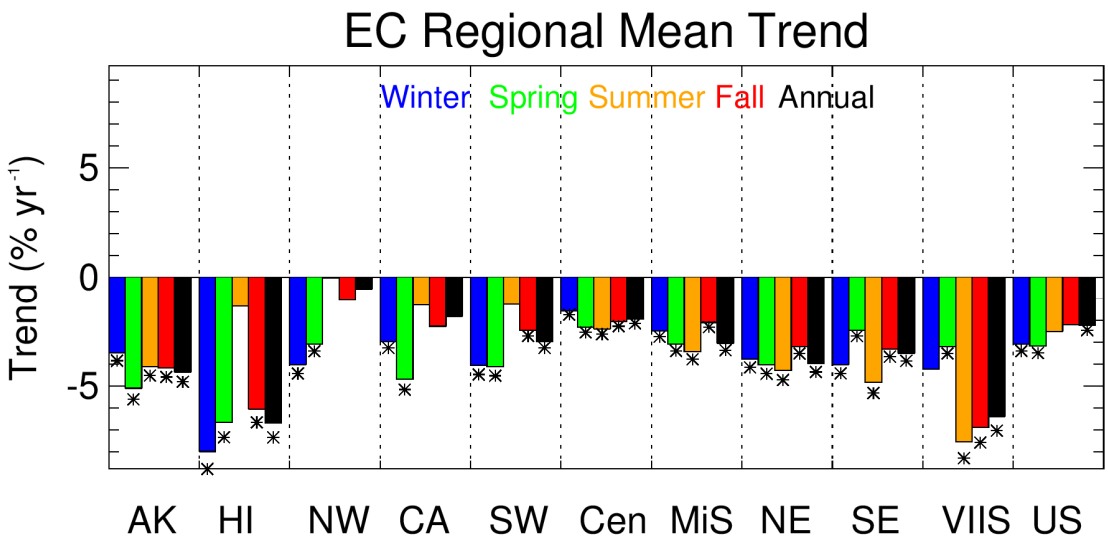


Figure 12. Regional, seasonal mean elemental carbon (EC) trends (% $yr^{-1}$) from 2002–2021 for major U.S. regions for winter, spring, summer, fall, and annual means. Regions are arranged from west to east (AK = Alaska, HI = Hawaii, NW = Northwest, CA= California, SW = Southwest, Cen = Central, MiS = Midsouth, NE = Northeast, SE = Southeast, VIIS = Virgin Islands, and US = all sites). Statistically significant trends ($p \leq 0.05$) are denoted with "*".

*4.6 Fine Dust*

Seasonal mean trends in FD demonstrated a high degree of spatial variability (Figure 13a-d), and had the fewest number of sites with statistically significant trends of any species. The strongest reductions in FD occurred during winter at sites in the eastern United States (Figure 13a), around -5% $yr^{-1}$ to -6% $yr^{-1}$. Unlike the east-west gradients seen in spatial patterns of trends for other species, FD winter mean trends had a north-south gradient (similar to Figure 2e), with negative trends at sites in the Northwest and Northern Great Plains, but insignificant trends at sites across California and the Southwest. Trends in spring (Figure 13b) were generally less negative than during winter across the United States, with some exceptions, including sites in Arizona, Washington, Montana, and North Dakota. Winter and spring CONUS trends ranged from -6.7% $yr^{-1}$ ($p < 0.001$) in Mohawk Mountain, Connecticut (MOMO1) to -1.5% $yr^{-1}$ ($p = 0.028$) in Martha's Vineyard, Massachusetts (MAVI1). Most of the trends in summer and fall were insignificant, especially at sites in the central and western United States (Figure 13c and 13d,

603 respectively), where several local and regional dust sources exist (Ginoux et al., 2012).
604 Insignificant trends at sites in the Northern Great Plains were likely associated with oil and gas
605 development, as these sites also had insignificant trends in nitrate, OC, and EC. Statistically
606 significant positive trends occurred in both summer and fall. In summer, seven sites had positive
607 trends, with the highest (>2% $yr^{-1}$) at Mount Hood, Oregon (2.3% $yr^{-1}$, $p = 0.040$, MOHO1),
608 Medicine Lake, Montana (2.9% $yr^{-1}$, $p = 0.001$, MELA1), and Three Sisters, Oregon (4.2% $yr^{-1}$,
609 $p = 0.017$, THSI1). During fall, statistically significant positive trends occurred at two sites,
610 including Dome Lands, California (2.7% $yr^{-1}$, $p = 0.025$, DOME1) and Zion Canyon, Utah (4.7%
611 $yr^{-1}$, $p = 0.021$, ZICA1). Summer trends at sites in the Southeast were insignificant.

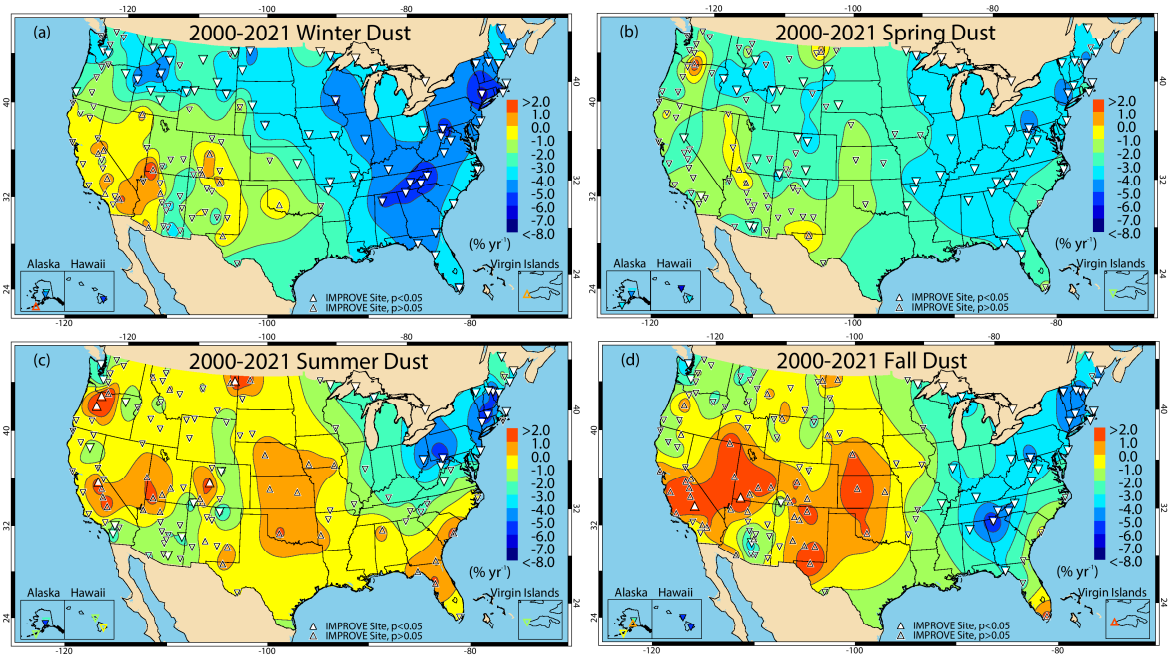


612
613 Figure 13. Seasonal mean fine dust (FD) trends (% $yr^{-1}$) from 2000–2021 for (a) winter (DJF) (b)
614 spring (MAM) (c) summer (JJA), and (d) fall (SON). Filled triangles correspond to statistically
615 significant trends ($p \leq 0.05$).

616 Regional, seasonal mean FD trends were mostly insignificant and generally less negative
617 compared to other species (Figure 14). Only the Northeast region had statistically significant
618 negative trends during all seasons, with the strongest reduction in winter (-5.1% $yr^{-1}$, $p < 0.001$).
619 The Southeast region had statistically significant reductions in FD during winter and spring and a
620 flat trend during summer, when transport of North African dust regularly influences sites in the
621 region. Similarly, the Midsouth region had insignificant but positive trends during summer. In

the Central region, only winter and spring had statistically significant negative trends (~-2% $yr^{-1}$); summer, fall, and annual mean trends were insignificant. Across the West, regions had insignificant though negative or flat trends. The California region had insignificant but positive trends during fall, and the summer trends in the Northwest region was flat. Many of the seasonal mean trends in the OCONUS regions were insignificant, except for spring, summer and annual mean trends in the Alaska region, and winter, fall, and annual mean trends in the Hawaii region. The annual mean FD trend across the United States was -1.3% $yr^{-1}$ ($p = 0.009$). FD has not experienced the levels of reduction as sulfate and nitrate, in part because dust has more natural sources and therefore its trends are less influenced by changes in anthropogenic emissions. FD timelines corresponding to the trends shown in Figure 14 can be found in Figures S26-S30.

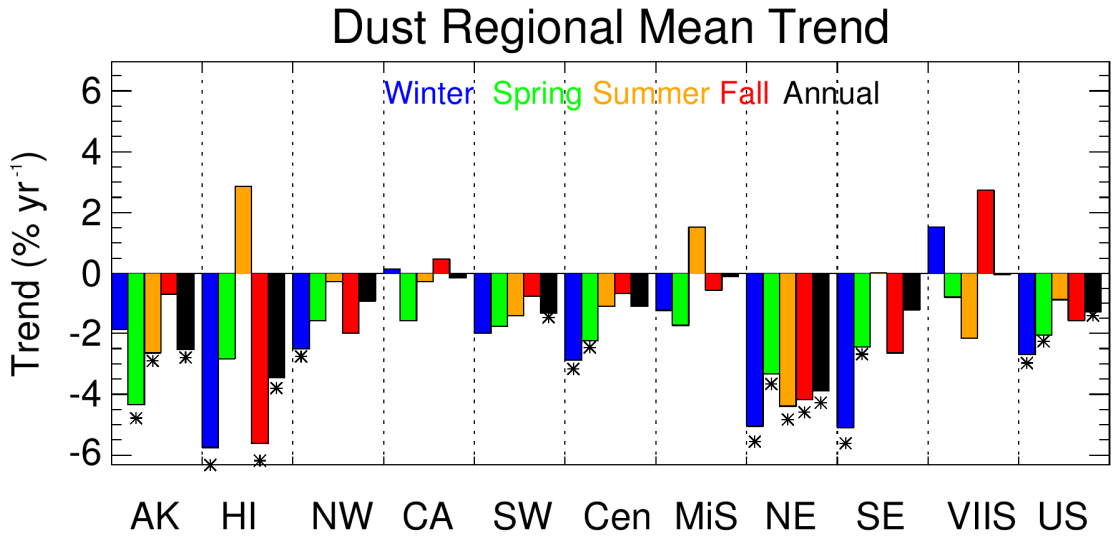


Figure 14. Regional, seasonal mean fine dust (FD) trends (% $yr^{-1}$) from 2002–2021 for major U.S. regions for winter, spring, summer, fall, and annual means. Regions are arranged from west to east (AK = Alaska, HI = Hawaii, NW = Northwest, CA= California, SW = Southwest, Cen = Central, MiS = Midsouth, NE = Northeast, SE = Southeast, VIIS = Virgin Islands, and US = all sites). Statistically significant trends ($p \leq 0.05$) are denoted with "*".

## 5.0 Discussion and Summary

Reductions in FM have occurred at nearly all remote regions across the United States. These reductions were strongest for regions in the East and were driven by negative trends in sulfate ion concentrations. Comparisons between trends in FM and sulfate showed similarities for all seasons at eastern regions. Sulfate concentrations have decreased in response to reductions in

$SO_2$ emissions due to regulatory activity. A timeline of the NEI total annual $SO_2$ emissions and U.S. annual mean sulfate concentrations is shown in Figure 15, with an inset of a scatter plot of $SO_2$ emissions and sulfate concentrations.

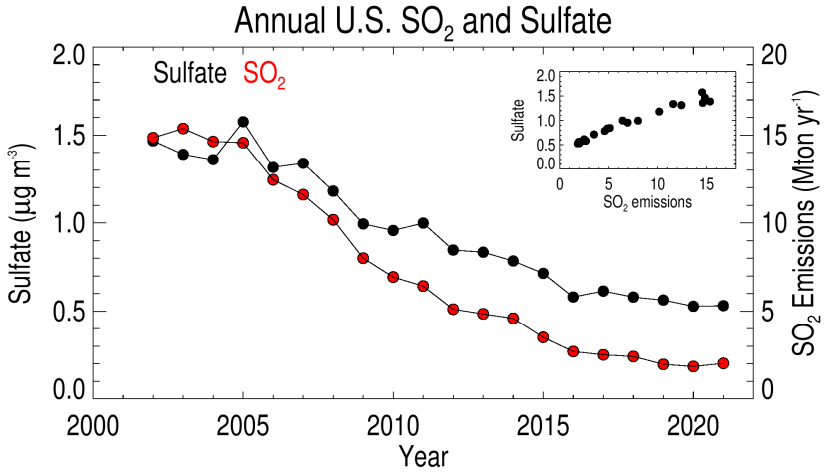


Figure 15. Total U.S. annual mean sulfate ion concentration (left axis, µg m-3) and NEI total annual $SO_2$ emissions (right axis, Mton $yr^{-1}$). The insert is a scatter plot of annual mean sulfate concentrations and $SO_2$ emissions (same units).

$SO_2$ emissions have declined by 87% between 2002 and 2021. $SO_2$ emissions and sulfate concentrations were highly correlated (r=0.98), and a linear Theil regression slope suggested a reduction of 0.070 ± 0.003 µg $m^{-3}$ of sulfate per Mton $yr^{-1}$ reduction of $SO_2$ emissions and an intercept of 0.48 ± 0.03 µg $m^{-3}$ corresponding to a "background" sulfate concentration (± one standard error). These values were similar to those reported by Hand et al., (2020) (slope of 0.072 ± 0.005 µg $m^{-3}$ per Mton $yr^{-1}$ and intercept of 0.51 ± 0.05 µg $m^{-3}$) for data from 2002 through 2018 at rural IMPROVE sites. Decreases in nitrate and OC concentrations in the eastern regions have also contributed to negative FM trends (e.g., Hidy et al., 2014; Blanchard et al., 2016; Malm et al., 2017; Ridley et al., 2018). As demonstrated in Figure 1, these species contribute a larger fraction of FM now than they did two decades ago in large part due to the reductions in sulfate.

The impacts of nitrate trends on FM were not as obvious, except for the southern California region during the winter season. Figure 1(d) shows that nitrate has declined on an annual basis in the California region, likely due to reductions in NOx mobile emissions (Yu et al., 2021).

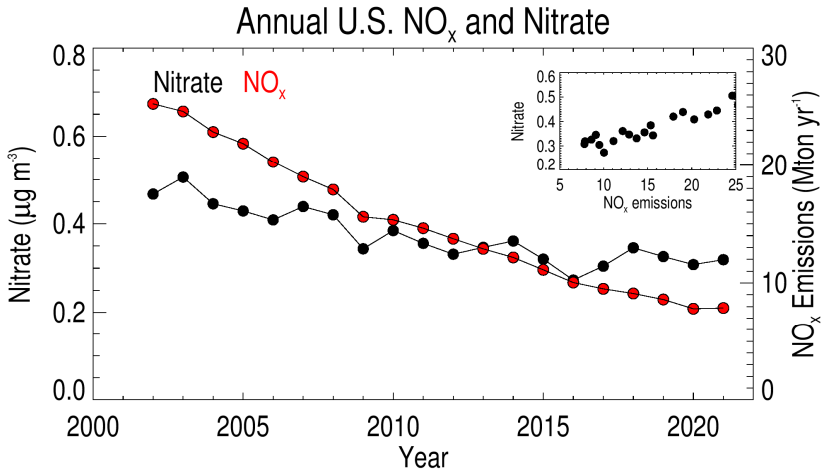


Figure 16. Total U.S. annual mean nitrate ion concentration (left axis, µg m-3) and NEI total annual NOx emissions (right axis, Mton $yr^{-1}$). The insert is a scatter plot of annual mean nitrate concentrations and NOx emissions (same units).

As shown in Figure 16, NOx emissions have dropped by 70% from 2002 to 2021. NOx emissions and annual mean nitrate concentrations were highly correlated ($r=0.93$, $p<0.001$) and a linear Theil regression resulted in a slope of $0.010 \pm 0.001$ µg $m^{-3}$ per Mton $yr^{-1}$ emissions, suggesting that on average the response of nitrate concentrations to NOx emission reductions was not as strong as for sulfate. One possible explanation is that particulate nitrate formation was ammonia-limited in many rural areas of the United States. With the decrease in sulfate, more ammonia is available to neutralize nitric acid. Declines in NOx emissions make this is less true today (e.g., Feng et al., 2020). An intercept of $0.21 \pm 0.02$ µg $m^{-3}$ also suggested missing sources of NOx in the emission inventory, including oil and gas and agricultural emissions (Thompson et al., 2017; Gebhart et al., 2018; Pozzer et al., 2017; Dix et al., 2020). These results agreed with previous estimates from Hand et al. (2020) for 2002 through 2018 (slope of $0.014 \pm 0.002$ µg $m^{-3}$ per Mton $yr^{-1}$ and intercept of $0.16 \pm 0.03$ µg $m^{-3}$). Nitrate contributes significantly to FM in the Central U.S. region (Figure 1), and agricultural sources of nitrate are important in this regions (Pitchford et al., 2009; Pozzer et al., 2017).

FM has declined at a weaker rate in regions in the West relative to eastern regions, especially during summer and fall. The flat and insignificant trends in OC, as well as reductions in other species, have led to greater contributions of OC to FM over time in western regions (recall Figures 1d, 1e, and 1f). As a result, FM trends at sites in the West were influenced by seasonal mean trends in OC concentrations, especially in summer and fall, as indicated by similarities in

their trends. The summer and fall seasons were most impacted by biomass smoke emissions, and the impacts of high fire years were especially evident on OC concentrations for 2017–2018, and 2020–2021 (see Figure 1d). A comparison of total U.S. wildland burn area and total U.S. annual mean OC concentrations are shown in Figure 17a, with a correlation coefficient of r = 0.47 (p = 0.032). Burn area includes contributions from the entire U.S. and not all OC is due to fire emissions, so it is only a rough comparison. Comparing annual mean OC concentrations from only the Northwest region to total annual burn area increased the correlation to r = 0.52 (p = 0.016). After 2015, total annual OC concentrations follow burn area more closely. In contrast to the West, seasonal mean OC concentrations in eastern regions decreased significantly for all seasons. Total annual NEI VOC emissions are shown with annual mean OC concentrations in Figure 17b, with an inset of VOC emissions and OC concentrations. The correlation coefficient was r = 0.89 ($p < 0.001$), much higher than for OC and burn area. However, the fraction of VOC emissions due to wildfires has increased over the last two decades, from 8% in 2002 to 28% in 2021. Malm et al., (2017) also showed a high likelihood that much of the reduction in OC in the East in summer and fall can be attributed to reduced sulfate concentrations and sulfate catalyzed OC formation.

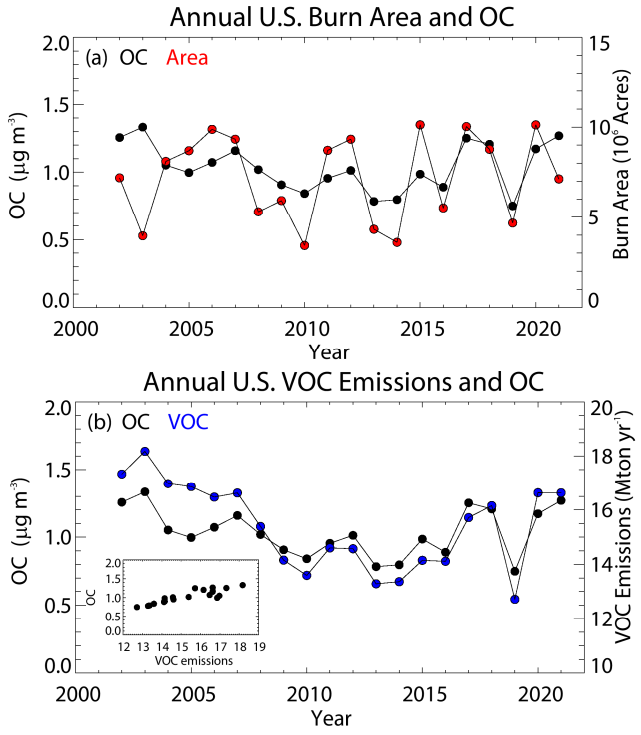

Figure 17 (a) Total U.S. annual mean organic carbon (OC) concentration (left axis, µg $m^{-3}$) and total U.S. wildland fire burn area (right axis, $10^6$ acres) (b) total U.S. annual mean OC concentration (left axis, µg $m^{-3}$) and total annual U.S. NEI volatile organic carbon (VOC) emissions (right axis, Mton $yr^{-1}$).

In the Southwest, OC and sulfate contributed similar fractions to FM on an annual basis (Figure 1e), but the major contribution came from FD. FD trends in the region have been linked to meteorological conditions such as drought (Achakulwisut et al., 2019) and large-scale climate variability (Hand et al., 2016; Pu and Ginoux, 2018). For example, the negative phase of the PDO has been associated with drought in the Southwest (e.g., Weiss et al. 2009). Hand et al., (2016) identified an inverse relationship between regional, March monthly mean FD in the Southwest and the March PDO index from 1995 through 2014 (r = -0.65). Later years were included here to compare Southwest regional, spring mean FD and March PDO indices from 2002 through 2021 (Figure 18). The y-axis for the PDO index is reversed as negative PDO indices tend to correspond to higher FD concentrations. A correlation coefficient of r = -0.46 (p = 0.032) suggested that the PDO has influence on the seasonal FD concentrations in the region.

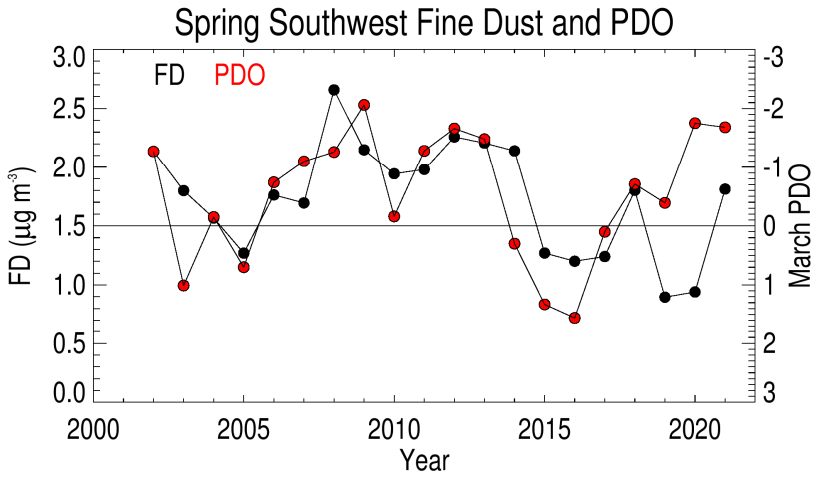


Figure 18. Southwest spring (MAM) mean fine dust (FD) concentrations (left-axis, µg $m^{-3}$) and the March PDO index (right axis, reversed).

Overall, annual mean FM trends decreased at a statistically significant rate of -1.8% $yr^{-1}$. For individual species, sulfate had the strongest statistically significant reduction in total annual mean U.S. concentrations (-6.1% $yr^{-1}$), followed by nitrate (-2.7% $yr^{-1}$), and EC (-2.2% $yr^{-1}$). The lowest reductions corresponded to FD (-1.3% $yr^{-1}$) and OC (-0.9% $yr^{-1}$), although the annual mean OC trend was insignificant. While OC decreased significantly across sites in the East, likely due to successful regulatory activity, OC trends at regions in the West were flat and

insignificant during seasons influenced by biomass burning emissions. OC is a major contributor to FM in the West and contributed to flat and insignificant trends in FM in similar regions during summer and fall. This influence will likely hinder future progress in FM reductions, especially in the West. The lessons learned regarding successful regulatory activity that resulted in reduced FM and speciated composition could be applied to managing other unregulated anthropogenic sources, such as oil and gas and agricultural emissions, because, as regulated precursors continue to decline, other sources will grow in importance. These sources include unregulated anthropogenic sources, as well as natural sources such as wildfire and dust, which are also predicted to increase with climate change.


## Acknowledgments

This work was funded by the National Park Service Air Resources Division under task agreement number P21AC11375-03 under Cooperative Agreement P17AC00971 and views presented herein are those of the authors and should not be interpreted as necessarily representing the National Park Service. IMPROVE is a collaborative association of state, tribal, and federal agencies, and international partners. The U.S. Environmental Protection Agency (EPA) is the primary funding source, with contracting and research support from the National Park Service. The Air Quality Group at the University of California, Davis, is the central analytical laboratory, with ion analysis provided by the Research Triangle Institute and carbon analysis provided by the Desert Research Institute.


## Conflict of Interest

The authors declare no conflicts of interest relevant to this study.

## Data Contributions:

Conceptualization: J. L. Hand, A. J. Prenni, B. A. Schichtel
Formal analysis: J. L. Hand
Methodology: J. L. Hand, A. J. Prenni, B. A. Schichtel
Visualization: J. L. Hand
Writing- original draft: J. L. Hand
Writing- review: A. J. Prenni, B. A. Schichtel

## Data Availability Statement

These datasets are publicly available, as follows:

IMPROVE: Federal Land Manager Environmental Database (http://views.cira.colostate.edu/fed/)
EPA National Emission Inventory (https://www.epa.gov/air-emissions-inventories/air-pollutant-emissions-trends-data)

National Interagency Fire Center (https://www.nifc.gov/fire-information/statistics/wildfires)
Pacific Decadal Oscillation Index from the National Centers for Environmental Information (NCEI) (https://www.ncei.noaa.gov/access/monitoring/pdo/).

**References**


Achakulwisut, P., S. C. Anenberg, J. E. Neumann, S. L. Penn, N. Weiss, A. Crimmins, N. Fann, J. Martinich, H. Roman, and L. J. Mickley (2019), Effects of increasing aridity on ambient dust and public health in the US Southwest under climate change, *GeoHealth*, *3*(5), 127-144, doi:https://doi.org/10.1029/2019GH000187.

Aldhaif, A. M., D. H. Lopez, H. Dadashazar, and A. Sorooshian (2020), Sources, frequency, and chemical nature of dust events impacting the United States East Coast, *Atmospheric Environment*, *231*, 12, doi:10.1016/j.atmosenv.2020.117456.

Attwood, A., R. Washenfelder, C. Brock, W. Hu, K. Baumann, P. Campuzano-Jost, D. Day, E. Edgerton, D. Murphy, and B. Palm (2014), Trends in sulfate and organic aerosol mass in the Southeast US: Impact on aerosol optical depth and radiative forcing, *Geophysical Research Letters*, *41*(21), 7701-7709, doi:doi:10.1002/2014GL061669.

Beachley, G., M. Phuchalski, C. Rogers, and G. Lear (2016), A summary of long-term trends in sulfur and nitrogen deposition in the United States 1990–2013, *JSM Environmental Science & Ecology*, *4*(2), 1030.

Benedict, K. B., A. J. Prenni, M. M. El-Sayed, A. Hecobian, Y. Zhou, K. A. Gebhart, B. C. Sive, B. A. Schichtel, and J. L. Collett Jr (2020), Volatile organic compounds and ozone at four national parks in the southwestern United States, *Atmospheric Environment*, *239*, 117783, doi:https://doi.org/10.1016/j.atmosenv.2020.117783.

Blanchard, C., G. Hidy, S. Tanenbaum, E. Edgerton, and B. Hartsell (2013), The Southeastern Aerosol Research and Characterization (SEARCH) study: Temporal trends in gas and PM concentrations and composition, 1999–2010, *Journal of the Air & Waste Management Association*, *63*(3), 247-259, doi:doi:10.1080/10962247.2012.748523.

Blanchard, C., G. Hidy, S. Shaw, K. Baumann, and E. Edgerton (2016), Effects of emission reductions on organic aerosol in the southeastern United States, *Atmospheric Chemistry and Physics*, *16*(1), 215-238, doi:doi:10.5194/acp-16-215-2016.

Bond, T. C., S. J. Doherty, D. W. Fahey, P. M. Forster, T. Berntsen, B. J. DeAngelo, M. G. Flanner, S. Ghan, B. Kärcher, and D. Koch (2013), Bounding the role of black carbon in

795 the climate system: A scientific assessment, *Journal of Geophysical Research:*
796 *Atmospheres*, *118*(11), 5380-5552, doi:doi:10.1002/jgrd.50171.
797 Bozlaker, A., J. M. Prospero, J. Price, and S. Chellam (2019), Identifying and quantifying the
798 impacts of advected North African dust on the concentration and composition of airborne
799 fine particulate matter in Houston and Galveston, Texas, *Journal of Geophysical Research:*
800 *Atmospheres*, *124*(22), 12282-12300, doi:https://doi.org/10.1029/2019JD030792.
801 Chan, E. A. W., B. Gantt, and S. McDow (2018), The reduction of summer sulfate and switch
802 from summertime to wintertime PM2.5 concentration maxima in the United States,
803 *Atmospheric Environment*, *175*, 25-32, doi:10.1016/j.atmosenv.2017.11.055.
804 Chen, Y., H. Shen, and A. G. Russell (2019), Current and future responses of aerosol ph and
805 composition in the US to declining SO2 emissions and increasing NH3 emissions,
806 *Environmental Science & Technology*, *53*(16), 9646-9655, doi:DOI:
807 10.1021/acs.est.9b02005.
808 Chow, J. C., J. G. Watson, D. H. Lowenthal, and K. L. Magliano (2005), Loss of PM2.5 Nitrate
809 from Filter Samples in Central California, *Journal of the Air & Waste Management*
810 *Association*, *55*(8), 1158-1168, doi:10.1080/10473289.2005.10464704.
811 Chow, J. C., J. G. Watson, L.-W. A. Chen, M. O. Chang, N. F. Robinson, D. Trimble, and S.
812 Kohl (2007), The IMPROVE_A temperature protocol for thermal/optical carbon analysis:
813 maintaining consistency with a long-term database, *Journal of the Air & Waste*
814 *Management Association*, *57*(9), 1014-1023, doi:https://doi.org/10.3155/1047-
815 3289.57.9.1014.
816 Chow, J., J. Watson, L.-W. Chen, J. Rice, and N. Frank (2010), Quantification of PM 2.5 organic
817 carbon sampling artifacts in US networks, *Atmospheric Chemistry and Physics*, *10*(12),
818 5223-5239, doi:https://doi.org/10.5194/acp-10-5223-2010.
819 Creamean, J. M., J. R. Spackman, S. M. Davis, and A. B. White (2014), Climatology of long-
820 range transported Asian dust along the West Coast of the United States, *Journal of*
821 *Geophysical Research: Atmospheres*, *119*(21), 12,171-112,185,
822 doi:doi:10.1002/2014JD021694.
823 Debell, L. J. (2006), Data Validation Historical Report NO3, .
824 http://vista.cira.colostate.edu/improve/wp-

825 content/uploads/2022/09/044_Historical_QA_Report_Nitrate.pdf, accessed 24 August
826 2023.
827 Dix, B., et al. (2020), Nitrogen Oxide Emissions from US Oil and Gas Production: Recent
828 Trends and Source Attribution, *Geophysical Research Letters*, *47*(1), 9,
829 doi:10.1029/2019gl085866.
830 Du, E., W. de Vries, J. N. Galloway, X. Hu, and J. Fang (2014), Changes in wet nitrogen
831 deposition in the United States between 1985 and 2012, *Environmental Research Letters*, *9*,
832 095004, doi:doi:10.1088/1748-9362/9/9/095004.
833 Ellis, R., D. J. Jacob, M. P. Sulprizio, L. Zhang, C. Holmes, B. Schichtel, T. Blett, E. Porter, L.
834 Pardo, and J. Lynch (2013), Present and future nitrogen deposition to national parks in the
835 United States: Critical load exceedances, *Atmospheric Chemistry and Physics*, *13*(17),
836 9083-9095, doi:doi:10.5194/acp-13-9038-2013.
837 Evanoski-Cole, A., K. Gebhart, B. Sive, Y. Zhou, S. Capps, D. Day, A. Prenni, M. Schurman, A.
838 Sullivan, and Y. Li (2017), Composition and sources of winter haze in the Bakken oil and
839 gas extraction region, *Atmospheric Environment*, *156*, 77-87,
840 doi:http://dx.doi.org/10.1016/j.atmosenv.2017.02.019.
841 Feng, J., E. Chan, and R. Vet (2020), Air quality in the eastern United States and eastern Canada
842 for 1990–2015: 25 years of change in response to emission reductions of SO2 and NOx in
843 the region, *Atmospheric Chemistry and Physics*, *20*(5), 3107-3134, doi:doi:10.5194/acp-20-
844 3107-2020.
845 Field, J. P., J. Belnap, D. D. Breshears, J. C. Neff, G. S. Okin, J. J. Whicker, T. H. Painter, S.
846 Ravi, M. C. Reheis, and R. L. Reynolds (2010), The ecology of dust, *Frontiers in Ecology*
847 *and the Environment*, *8*(8), 423-430, doi:doi:10.1890/090050.
848 Frank, N. H. (2006), Retained nitrate, hydrated sulfates, and carbonaceous mass in federal
849 reference method fine particulate matter for six eastern US cities, *Journal of the Air &*
850 *Waste Management Association*, *56*(4), 500-511,
851 doi:https://doi.org/10.1080/10473289.2006.10464517.
852 Gebhart, K. A., D. E. Day, A. J. Prenni, B. A. Schichtel, J. L. Hand, and A. R. Evanoski-Cole
853 (2018), Visibility impacts at Class I areas near the Bakken oil and gas development,
854 *Journal of the Air & Waste Management Association*, *68*(5), 477-493,
855 doi:10.1080/10962247.2018.1429334.

856 Ginoux, P., J. M. Prospero, T. E. Gill, N. C. Hsu, and M. Zhao (2012), Global-scale attribution
857 of anthropogenic and natural dust sources and their emission rates based on MODIS Deep
858 Blue aerosol products, *Reviews of Geophyics, 50,* RG3005, doi:10.1029/2012RG000388.
859 Hand, J. L., B. A. Schichtel, W. C. Malm, and M. L. Pitchford (2012a), Particulate sulfate ion
860 concentration and SO2 emission trends in the United States from the early 1990s through
861 2010, *Atmospheric Chemistry and Physics*, *12*(21), 10353-10365, doi:doi:10.5194/acp-12-
862 10353-2012.
863 Hand, J. L., K. A. Gebhart, B. A. Schichtel, and W. C. Malm (2012b), Increasing trends in
864 wintertime particulate sulfate and nitrate ion concentrations in the Great Plains of the
865 United States (2000-2010), *Atmospheric Environment*, *55*, 107-110,
866 doi:10.1016/j.atmosenv.2012.03.050.
867 Hand, J. L., B. A. Schichtel, W. C. Malm, S. Copeland, J. V. Molenar, N. H. Frank, and M.
868 Pitchford (2014), Widespread reductions in haze across the United States from the early
869 1990s through 2011, *Atmospheric Environment*, *94*, 671-679,
870 doi:doi:10.1016/j.atmosenv.2014.05.062.
871 Hand, J. L., W. White, K. Gebhart, N. Hyslop, T. Gill, and B. Schichtel (2016), Earlier onset of
872 the spring fine dust season in the southwestern United States, *Geophysical Research*
873 *Letters*, *43*(8), 4001-4009, doi:doi:10.1002/2016GL068519.
874 Hand, J. L., T. Gill, and B. Schichtel (2017), Spatial and seasonal variability in fine mineral dust
875 and coarse aerosol mass at remote sites across the United States, *Journal of Geophysical*
876 *Research: Atmospheres*, *122*(5), 3080-3097, doi:doi:10.1002/2016JD026290.
877 Hand, J. L., A. J. Prenni, B. A. Schichtel, W. C. Malm, and J. C. Chow (2019), Trends in remote
878 PM2.5 residual mass across the United States: Implications for aerosol mass reconstruction
879 in the IMPROVE network, *Atmospheric Environment*, *203*, 141-152,
880 doi:doi:10.1016/j.atmosenv.2019.01.049.
881 Hand, J. L., A. J. Prenni, S. Copeland, B. A. Schichtel, and W. C. Malm (2020), Thirty years of
882 the Clean Air Act Amendments: Impacts on haze in remote regions of the United States
883 (1990–2018), *Atmospheric Environment*, *243*, 117865,
884 doi:https://doi.org/10.1016/j.atmosenv.2020.117865.
885 Hand, J. L., et al. (2023), IMPROVE (Interagency Monitoring of Protected Visual
886 Environments): Spatial and seasonal patterns and temporal variability of haze and its

887 constituents in the United States, *IMPROVE Report VI*, Cooperative Institute for Research
888 in the Atmosphere, Colorado State University, Fort Collins, Colorado.,
889 http://vista.cira.colostate.edu/Improve/spatial-and-seasonal-patterns-and-temporal-
890 variability-of-haze-and-its-constituents-in-the-united-states-report-vi-june-2023/, Accessed
891 24 August 2023.

892 Heald, C., et al. (2012), Atmospheric ammonia and particulate inorganic nitrogen over the
893 United States, *Atmospheric Chemistry and Physics 12*, 10295-10312, doi:doi:10.5194/acp-
894 12-10295-2012.
895 Hering, S., and G. Cass (1999), The magnitude of bias in the measurement of PM25 arising from
896 volatilization of particulate nitrate from Teflon filters, *Journal of the Air & Waste*
897 *Management Association*, *49*(6), 725-733, doi:10.1080/10473289.1999.10463843.
898 Hidy, G., C. Blanchard, K. Baumann, E. Edgerton, S. Tanenbaum, S. Shaw, E. Knipping, I.
899 Tombach, J. Jansen, and J. Walters (2014), Chemical climatology of the southeastern
900 United States, 1999–2013, *Atmospheric Chemistry and Physics*, *14*(21), 11893-11914,
901 doi:doi:10.5194/acp-14-11893-2014.
902 Hu, C., T. J. Griffis, J. M. Baker, J. D. Wood, D. B. Millet, Z. Yu, and X. Lee (2020), Modeling
903 the sources and transport processes during extreme ammonia episodes in the US Corn Belt,
904 *Journal of Geophysical Research: Atmospheres*, *125*(2), e2019JD031207,
905 doi:https://doi.org/10.1029/2019JD031207.
906 Husar, R. B., D. Tratt, B. A. Schichtel, S. Falke, F. Li, D. Jaffe, S. Gasso, T. Gill, N. S.
907 Laulainen, and F. Lu (2001), Asian dust events of April 1998, *Journal of Geophysical*
908 *Research: Atmospheres*, *106*(D16), 18317-18330.
909 Hyslop, N. P., K. Trzepla, and W. H. White (2015), Assessing the suitability of historical PM2. 5
910 element measurements for trend analysis, *Environmental Science & Technology*, *49*(15),
911 9247-9255, doi:DOI: 10.1021/acs.est.5b01572.
912 Isaaks, E. H., and R. Mohan Srivastava (1989), *An Introduction to Applied Geostatistics*, Oxford
913 University Press, New York.
914 Kharol, S. K., C. A. McLinden, C. E. Sioris, M. W. Shephard, V. Fioletov, A. van Donkelaar, S.
915 Philip, and R. V. Martin (2017), OMI satellite observations of decadal changes in ground-
916 level sulfur dioxide over North America, *Atmospheric Chemistry and Physics*, *17*(9), 5921-
917 5929, doi:doi:10.5194/acp-17-5921-2017.

Kim, P. S., D. J. Jacob, J. A. Fisher, K. Travis, K. Yu, L. Zhu, R. M. Yantosca, M. Sulprizio, J. L. Jimenez, and P. Campuzano-Jost (2015), Sources, seasonality, and trends of southeast US aerosol: an integrated analysis of surface, aircraft, and satellite observations with the GEOS-Chem chemical transport model, *Atmospheric Chemistry and Physics*, *15*(18), 10411-10433, doi:doi:10.5194/acp-15-10411-2015.

Kim, D., M. Chin, C. A. Cruz, D. Tong, and H. Yu (2021), Spring dust in western north America and its interannual variability—understanding the role of local and transported dust, *Journal of Geophysical Research: Atmospheres*, *126*(22), e2021JD035383, doi:https://doi.org/10.1029/2021JD035383.

Krotkov, N. A., et al. (2016), Aura OMI observations of regional SO2 and NO2 pollution changes from 2005 to 2015, *Atmospheric Chemistry and Physics*, *16*(7), 4605-4629, doi:10.5194/acp-16-4605-2016.

Lambert, A., A. G. Hallar, M. Garcia, C. Strong, E. Andrews, and J. L. Hand (2020), Dust impacts of rapid agricultural expansion on the Great Plains, *Geophysical Research Letters*, *47*(20), e2020GL090347, doi:https://doi.org/10.1029/2020GL090347.

Lawal, A. S., X. Guan, C. Liu, L. R. Henneman, P. Vasilakos, V. Bhogineni, R. J. Weber, A. Nenes, and A. G. Russell (2018), Linked response of aerosol acidity and ammonia to SO2 and NOx emissions reductions in the United States, *Environmental Science & Technology*, *52*(17), 9861-9873, doi:doi:10.1021/acs.est.8b00711.

Lehmann, C. M., and D. A. Gay (2011), Monitoring long-term trends of acidic wet deposition in US precipitation: Results from the National Atmospheric Deposition Program, *PowerPlant Chemistry*, *13*(7), 378-385.

Lowenthal, D., and N. Kumar (2006), Light scattering from sea-salt aerosols at Interagency Monitoring of Protected Visual Environments (IMPROVE) sites, *Journal of the Air & Waste Management Association*, *56*(5), 636-642, doi:https://doi.org/10.1080/10473289.2006.10464478.

Lowenthal, D., B. Zielinska, V. Samburova, D. Collins, N. Taylor, and N. Kumar (2015), Evaluation of assumptions for estimating chemical light extinction at US national parks, *Journal of the Air & Waste Management Association*, *65*(3), 249-260, doi:10.1080/10962247.2014.986307.

948 Malm, W. C., J. F. Sisler, D. Huffman, R. A. Eldred, and T. A. Cahill (1994), Spatial and
949 seasonal trends in particle concentration and optical extinction in the United States, *Journal*
950 *of Geophysical Research: Atmospheres*, *99*(D1), 1347-1370, doi:
951 https://doi.org/10.1029/93JD02916.
952 Malm, W. C., B. A. Schichtel, R. B. Ames, and K. A. Gebhart (2002), A 10-year spatial and
953 temporal trend of sulfate across the United States, *Journal of Geophysical Research:*
954 *Atmospheres*, *107*(D22), 4627, doi:doi:10.1029/2002JD002107.
955 Malm, W. C., B. A. Schichtel, J. L. Hand, and J. L. Collett Jr (2017), Concurrent temporal and
956 spatial trends in sulfate and organic mass concentrations measured in the IMPROVE
957 monitoring program, *Journal of Geophysical Research: Atmospheres*, *122*, 10462-10476,
958 doi:https:/doi.org/10.1002/2017JD026865.
959 Malm, W., B. Schichtel, J. Hand, and A. Prenni (2020), Implications of organic mass to carbon
960 ratios increasing over time in the rural United States, *Journal of Geophysical Research:*
961 *Atmospheres*, *125*(5), e2019JD031480.
962 McClure, C. D., and D. A. Jaffe (2018), US particulate matter air quality improves except in
963 wildfire-prone areas, *Proceedings of the National Academy of Sciences*, *115*(31), 7901-
964 7906, doi:doi:10.1073/pnas.1804353115.
965 McDade, C. (2004), Summary of IMPROVE nitrate measurements,
966 http://vista.cira.colostate.edu/improve/Publications/GrayLit/025_IMPROVEnitrate/Nitrate
967 %20Summary_1004.pdf, accessed 24 August 2023.
968 McDade, C. (2007), Diminished wintertime nitrate concentrations in late 1990s, *IMPROVE Data*
969 *Advisory Document* #da0002.
970 http://vista.cira.colostate.edu/improve/Data/QA_QC/Advisory/da0002/da0002_WinterNO3
971 .pdf, accessed 24 August 2023.
972 Murphy, D. M., J. C. Chow, E. M. Leibensperger, W. C. Malm, M. Pitchford, B. A. Schichtel, J.
973 G. Watson, and W. H. White (2011), Decreases in elemental carbon and fine particle mass
974 in the United States, *Atmospheric Chemistry and Physics*, *11*(10), 4679-4686,
975 doi:10.5194/acp-11-4679-2011.
976 Murphy, D. M., et al. (2019), The distribution of sea-salt aerosol in the global troposphere,
977 *Atmospheric Chemistry and Physics*, *19*(6), 4093-4104, doi:10.5194/acp-19-4093-2019.

978 Naimie, L. E., A. P. Sullivan, K. B. Benedict, A. J. Prenni, B. C. Sive, B. A. Schichtel, E. V.
979 Fischer, I. Pollack, and J. Collett (2022), PM2.5 in Carlsbad Caverns National Park:
980 Composition, sources, and visibility impacts, *Journal of the Air & Waste Management*
981 *Association*, *72*(11), 1201-1218, doi:10.1080/10962247.2022.2081634.
982 Nopmongcol, U., R. Beardsley, N. Kumar, E. Knipping, and G. Yarwood (2019), Changes in
983 United States deposition of nitrogen and sulfur compounds over five decades from 1970 to
984 2020, *Atmospheric Environment*, *209*, 144-151,
985 doi:https://doi.org/10.1016/j.atmosenv.2019.04.018.
986 Park, R. J., D. J. Jacob, B. D. Field, R. M. Yantosca, and M. Chin (2004), Natural and
987 transboundary pollution influences on sulfate-nitrate-ammonium aerosols in the United
988 States: Implications for policy, *Journal of Geophysical Research: Atmospheres*, *109*,
989 D15204, doi:doi:10.1029/2003JD004473.
990 Park, R. J., D. J. Jacob, N. Kumar, and R. M. Yantosca (2006), Regional visibility statistics in
991 the United States: Natural and transboundary pollution influences, and implications for the
992 Regional Haze Rule, *Atmospheric Environment*, *40*(28), 5405-5423,
993 doi:10.1016/j.atmosenv.2006.04.059.
994 Paulot, F., S. Fan, and L. Horowitz (2017), Contrasting seasonal responses of sulfate aerosols to
995 declining SO2 emissions in the Eastern US: Implications for the efficacy of SO2 emission
996 controls, *Geophysical Research Letters*, *44*(1), 455-464, doi:doi:10.1002/2016GL070695.
997 Perry, K. D., T. A. Cahill, R. A. Eldred, D. D. Dutcher, and T. E. Gill (1997), Long-range
998 transport of North African dust to the eastern United States, *Journal of Geophysical*
999 *Research: Atmospheres*, *102*(D10), 11225-11238, doi: https://doi.org/10.1029/97JD00260.
1000 Petzold, A., et al. (2013), Recommendations for reporting "black carbon" measurements,
1001 *Atmospheric Chemistry and Physics*, *13*(16), 8365-8379, doi:10.5194/acp-13-8365-2013.
1002 Pitchford, M., R. Poirot, B. A. Schichtel, and W. C. Malm (2009), Characterization of the winter
1003 midwestern particulate nitrate bulge, *Journal of the Air & Waste Management Association*,
1004 *59*(9), 1061-1069, doi:doi:10.3155/1047-3289.59.9.1061.
1005 Pozzer, A., A. P. Tsimpidi, V. A. Karydis, A. de Meij, and J. Lelieveld (2017), Impact of
1006 agricultural emission reductions on fine-particulate matter and public health, *Atmospheric*
1007 *Chemistry and Physics*, *17*(20), 12813-12826, doi:10.5194/acp-17-12813-2017.

1008 Prenni, A., D. Day, A. Evanoski-Cole, B. Sive, A. Hecobian, Y. Zhou, K. Gebhart, J. Hand, A.
1009 Sullivan, and Y. Li (2016), Oil and gas impacts on air quality in federal lands in the
1010 Bakken region: an overview of the Bakken Air Quality Study and first results, *Atmospheric*
1011 *Chemistry and Physics*, *16*(3), 1401-1416, doi:doi:10.5194/acp-16-1401-2016.
1012 Prenni, A. J., et al. (2022), Wintertime haze and ozone at Dinosaur National Monument, *Journal*
1013 *of the Air & Waste Management Association*, *72*(9), 951-968,
1014 doi:10.1080/10962247.2022.2048922.
1015 Prospero, J. M., A. C. Delany, A. C. Delany, and T. N. Carlson (2021), The discovery of African
1016 dust transport to the Western Hemisphere and the Saharan air layer: a history, *Bulletin of*
1017 *the American Meteorological Society*, *102*(6), E1239-E1260,
1018 doi:https://doi.org/10.1175/BAMS-D-19-0309.1.
1019 Prospero, J. M., P. Ginoux, O. Torres, S. E. Nicholson, and T. E. Gill (2002), Environmental
1020 characterization of global sources of atmospheric soil dust identified with the Nimbus 7
1021 Total Ozone Mapping Spectrometer (TOMS) absorbing aerosol product, *Reviews of*
1022 *Geophysics*, *40*(1), 2-1-2-31, doi:1002, doi:10.1029/2000RG000095.
1023 Pu, B., and P. Ginoux (2018), Climatic factors contributing to long-term variations in surface
1024 fine dust concentration in the United States, *Atmospheric Chemistry and Physics*, *18*(6),
1025 4201-4215, doi:https://doi.org/10.5194/acp-18-4201-2018.
1026 Ridley, D. A., C. L. Heald, K. J. Ridley, and J. H. Kroll (2018), Causes and consequences of
1027 decreasing atmospheric organic aerosol in the United States, *Proceedings of the National.*
1028 *Academies of Science, 115*(2), 290-295, doi:10.1073/pnas.1700387115.
1029 Rivera, N. I. R., T. E. Gill, K. A. Gebhart, J. L. Hand, M. P. Bleiweiss, and R. M. Fitzgerald
1030 (2009), Wind modeling of Chihuahuan Desert dust outbreaks, *Atmospheric Environment*,
1031 *43*(2), 347-354, doi:doi:10.1016/j.atmosenv.2008.09.069.
1032 Russell, A., L. Valin, and R. Cohen (2012), Trends in OMI NO2 observations over the United
1033 States: Effects of emission control technology and the economic recession, *Atmospheric*
1034 *Chemistry and Physics*, *12*(24), 12197-12209, doi:doi:10.5194/acp-12-12197-2012.
1035 Samset, B. H., M. Sand, C. J. Smith, S. E. Bauer, P. M. Forster, J. S. Fuglestvedt, S. Osprey, and
1036 C. F. Schleussner (2018), Climate Impacts From a Removal of Anthropogenic Aerosol
1037 Emissions, *Geophysical Research Letters*, *45*(2), 1020-1029, doi:10.1002/2017gl076079.

Schichtel, B. A., M. L. Pitchford, and W. H. White (2011), Comments on "Impact of California's Air Pollution Laws on Black Carbon and their Implications for Direct Radiative Forcing" by R. Bahadur et al, *Atmospheric Environment*, *45*(24), 4116-4118, doi:doi:10.1016/j.atmosenv.2011.04.042.

Schichtel, B. A., W. C. Malm, M. Beaver, S. Copeland, J. L. Hand, A. J. Prenni, J. Rice, and J. Vimont (2021), The Future of Carbonaceous Aerosol Measurement in the IMPROVE Monitoring Program, http://vista.cira.colostate.edu/improve/wp-content/uploads/2021/10/041_CarbonReport_Final.pdf, last accessed 24 August 2023.

Seinfeld, J. H., et al. (2016), Improving our fundamental understanding of the role of aerosol-cloud interactions in the climate system, *Proceedings of the Natational Academies of Science*, *113*(21), 5781-5790, doi:10.1073/pnas.1514043113.

Shah, V., et al. (2018), Chemical feedbacks weaken the wintertime response of particulate sulfate and nitrate to emissions reductions over the eastern United States, *Proceedings of the Natational Academies of Science*, *115*(32), 8110-8115, doi:10.1073/pnas.1803295115.

Shi, Q. R., et al. (2022), Co-benefits of CO2 emission reduction from China's clean air actions between 2013-2020, *Nat. Commun.*, *13*(1), 8, doi:10.1038/s41467-022-32656-8.

Shiraiwa, M., et al. (2017), Aerosol Health Effects from Molecular to Global Scales, *Environmental Science & Technology*, *51*(23), 13545-13567, doi:10.1021/acs.est.7b04417.

Sickles, J. E., and D. S. Shadwick (2015), Air quality and atmospheric deposition in the eastern US: 20 years of change, *Atmospheric Chemistry and Physics 15*, 173-197, doi:doi:10.5194/acp-15-173-2015.

Silvern, R. F., D. J. Jacob, P. S. Kim, E. A. Marais, J. R. Turner, P. Campuzano-Jost, and J. L. Jimenez (2017), Inconsistency of ammonium–sulfate aerosol ratios with thermodynamic models in the eastern US: a possible role of organic aerosol, *Atmospheric Chemistry and Physics*, *17*(8), 5107-5118, doi:doi:10.5194/acp-17-5107-2017.

Theil, H. (1950), A rank-invariant method of linear and polynomial regression analysis., *Proc. Kon. Ned. Akad. v Wetensch.* , *A*(53), 386-392, doi:https://doi.org/10.1007/978094-011-2546-8_20.

Thompson, T. M., D. Shepherd, A. Stacy, M. G. Barna, and B. A. Schichtel (2017), Modeling to evaluate contribution of oil and gas emissions to air pollution, *Journal of the Air & Waste Management Association*, *67*(4), 445-461, doi:10.1080/10962247.2016.1251508.

1069 Tong, D., M. Dan, T. Wang, and P. Lee (2012), Long-term dust climatology in the western
1070 United States reconstructed from routine aerosol ground monitoring, *Atmospheric*
1071 *Chemistry and Physics*, *12*(11), 5189-5205, doi:doi:10.5194/acp-12-5189-2012.
1072 Vitousek, P. M., J. D. Aber, R. W. Howarth, G. E. Likens, P. A. Matson, D. W. Schindler, W. H.
1073 Schlesinger, and D. G. Tilman (1997), Human alteration of the global nitrogen cycle:
1074 sources and consequences, *Ecological Applications*, *7*(3), 737-750,
1075 doi:https://doi.org/10.1890/1051-0761(1997)007[0737:HAOTGN]2.0.CO;2.
1076 Warner, J., R. Dickerson, Z. Wei, L. Strow, Y. Wang, and Q. Liang (2017), Increased
1077 atmospheric ammonia over the world's major agricultural areas detected from space,
1078 *Geophysical Research Letters*, *44*, 2875-2884, doi:doi:10.1002/2016GL072305.
1079 Watson, J. G., J. C. Chow, L.-W. A. Chen, and N. H. Frank (2009), Methods to assess
1080 carbonaceous aerosol sampling artifacts for IMPROVE and other long-term networks,
1081 *Journal of the Air & Waste Management Association*, *59*(8), 898-911,
1082 doi:https://doi.org/10.3155/1047-3289.59.8.898.
1083 Weber, R. J., H. Guo, A. G. Russell, and A. Nenes (2016), High aerosol acidity despite declining
1084 atmospheric sulfate concentrations over the past 15 years, *Nature Geoscience*, *9*(4), 282-
1085 285, doi:DOI: 10.1038/NGEO2665.
1086 Weiss, J. L., C. L. Castro, and J. T. Overpeck (2009), Distinguishing Pronounced Droughts in the
1087 Southwestern United States: Seasonality and Effects of Warmer Temperatures, *Journal of*
1088 *Climate*, *22*(22), 5918-5932, doi:10.1175/2009jcli2905.1.
1089 White, W. H. (2006), Elemental concentrations of Al above the MDL can go undetected,
1090 *IMPROVE Data Advisory Document* #da0010,
1091 http://vista.cira.colostate.edu/improve/Data/QA_QC/Advisory/da0010/da0010_Almdl.pdf,
1092 last accessed 24 August 2023.
1093 White, W. H. (2007), Shift in EC/OC split with 1 January 2005 TOR hardware upgrade,
1094 *IMPROVE Data Advisory Document* #da0016,
1095 http://vista.cira.colostate.edu/improve/Data/QA_QC/Advisory/da0016/da0016_TOR2005.p
1096 df, last accessed 24 August 2023.
1097 White, W. H. (2008), Chemical markers for sea salt in IMPROVE aerosol data, *Atmospheric*
1098 *Environment*, *42*(2), 261-274, doi:doi:10.1016/j.atmosenv.2007.09.040.

White, W. H. (2016), Increased variation of humidity in the weighing laboratory, *IMPROVE Data Advisory Document* #da0035, http://vista.cira.colostate.edu/improve/Data/QA_QC/Advisory/da0035/da0035_IncreasedRH.pdf, last accessed 24 August 2023.

Yu, K. A., B. C. McDonald, and R. A. Harley (2021), Evaluation of Nitrogen Oxide Emission Inventories and Trends for On-Road Gasoline and Diesel Vehicles, *Environmental Science & Technology*, *55*(10), 6655-6664, doi:10.1021/acs.est.1c00586.

Zhang, Y., R. Mathur, J. O. Bash, C. Hogrefe, J. Xing, and S. J. Roselle (2018), Long-term trends in total inorganic nitrogen and sulfur deposition in the US from 1990 to 2010, *Atmospheric Chemistry and Physics*, *18*(12), 9091, doi:doi:10.5194/acp-18-9091-2018.

Zhang, X. (2019), Correction of chloride concentrations for filter blank levels, *IMPROVE Data Advisory Document* #da0039., http://vista.cira.colostate.edu/improve/Data/QA_QC/Advisory/da0039/da0039_ChlorideOverCorrection.pdf, last accessed 24 August 2023.